Copy No. 17
RM No. L7G25

NACA

16 NOV 1947

UNCLASSIFIED

RESEARCH MEMORANDUM

for the

Air Materiel Command, Army Air Forces

DEVELOPMENT OF OUTBOARD NACELLE FOR THE XB-36 AIRPLANE

By

Robert J. Nuber

Langley Memorial Aeronautical Laboratory
Langley Field, Va.

NATIONAL ADVISORY COMMITTEE
FOR AERONAUTICS

WASHINGTON

OCT 31 1947

NACA RM No. L7G25

NATIONAL ADVISORY COMMITTEE FOR AERONAUTICS

RESEARCH MEMORANDUM

for the

Air Materiel Command, Army Air Forces

DEVELOPMENT OF OUTBOARD NACELLE FOR THE XB-36 AIRPLANE

By Robert J. Nuber

SUMMARY

An investigation of two $\frac{1}{14}$-scale model configurations of an outboard nacelle for the XB-36 airplane was made in the Langley two-dimensional low-turbulence tunnels over a range of airplane lift coefficients (C_L = 0.409 to C_L = 0.943) for three representative flow conditions. The purpose of the investigation was to develop a low-drag wing-nacelle pusher combination which incorporated an internal air-flow system. The present investigation has led to the development of a nacelle which had external drag coefficients of similar order of magnitude to those obtained previously from tests of an inboard nacelle configuration at the corresponding operating lift coefficients and from approximately one-third to one-half of those of conventional tractor designs having the same ratio of wing thickness to nacelle diameter.

It was found that the total drag of nacelle configuration 2, in general, was lower than that of nacelle configuration 1 for the flight conditions investigated entirely because of the improvements made in the internal ducting system. At the simulated 40,000-foot climb condition, the external drag of nacelle configuration 2, corresponding to a lift coefficient of 0.912, was approximately 52 percent less than that of configuration 1 due to increasing the stagger angle and lip radii of the air inlets.

The results also indicated that the cooling fan might be required for the 40,000-foot cruise condition and almost certainly will be required for the 40,000-foot climb condition.

INTRODUCTION

A series of investigations were made in the Langley low-turbulence tunnels in an effort to develop satisfactory pusher-type

nacelles for the six-engine Consolidated heavy bomber designated XB-36, which incorporate ducting systems designed so that the cooling air is admitted at the wing leading edge. The results of one series of investigations, dealing with an inboard nacelle, have been presented in reference 1. The present investigation is concerned with the development of an outboard nacelle.

The findings of reference 1 were taken into consideration in the design of the initial outboard nacelle configuration. The basic design is similar to that given as configuration 3 of reference 1, but differed slightly from this configuration because of the smaller chord and thickness ratio of the wing. The nacelle was constructed to $\frac{1}{14}$ scale and was tested in conjunction with an NACA 63(420)-4(20.7) (approximate) airfoil at a Reynolds number of approximately 1.7×10^6 through the complete calculated flight range of lift coefficients for three representative flow conditions: namely, 10,000- and 40,000-foot cruise and 40,000-foot climb. The effects on external nacelle drag of refairing the nacelle upper surface and installing fillets in the wing-nacelle junctures were determined. It was found desirable from these proliminary tests to make several modifications in an effort to improve the flow over the nacelle and through the ducting system. These modifications consisted of changes to the air inlets and duct shapes. The resulting configuration was tested for the flow conditions previously indicated.

It is of interest to note that the nacelle configurations described herein differ in general appearance from those on the three-dimensional installation described in reference 2 due to wing sweepback, plan form, and thickness taper. The results presented in this paper, therefore, may be influenced by these factors.

COEFFICIENTS AND SYMBOLS

C_L airplane lift coefficient

c_l model lift coefficient

c_{l_a} airfoil section lift coefficient

c_{d_a} airfoil section drag coefficient

C_{D_F} nacelle total drag coefficient

[redacted]

C_{D_p} nacelle external drag coefficient $\left(C_{D_F} - C_{D_i}\right)$

C_{D_i} calculated drag coefficient caused by internal flow (exclusive of engine charge air)

α airplane angle of attack

α_m model angle of attack

α_a section angle of attack

q dynamic pressure $\left(\frac{\rho V^2}{2}\right)$

ρ mass density

V velocity measured at point of subscript

F model nacelle frontal area (38.2 sq in.)

Q volume rate of flow through duct

c model wing chord (16.37 in.)

R Reynolds number based on chord $\left(\frac{\rho_o V_o c}{\mu}\right)$

A duct cross-sectional area

$\frac{\Delta H}{q_o}$ average total-pressure defect coefficient

$\frac{\Delta P}{q_o}$ total-pressure loss coefficient across baffle

$\frac{V_n}{V_o}$ inlet-velocity ratio $\left(\frac{F}{A_n}\left(\frac{Q}{FV_o}\right)_n\right)$

μ coefficient of viscosity

Subscripts:

o in free stream

n in duct inlet

e in duct exit

[redacted]

MODEL AND APPARATUS

Both configurations discussed herein represented an outboard nacelle for the XB-36 airplane and were constructed to $\frac{1}{14}$ scale. The nacelle designed for pusher propellers had a frontal area of 38.2 square inches and was mounted on the center section of a 16.37-inch chord wing section of 36-inch span which was built to the contour of an NACA 63(420)-4(20.7) (approximate) airfoil which corresponds to the section at the center line of the nacelle. Ordinates for the plain airfoil, which was tested with and without the nacelle, are given in percent of airfoil chord in table I.

Configuration 1.- A general outline of the model is shown in figure 1. Cooling air for the engine and intercoolers entered the common duct at the wing leading edge while air for the oil cooler and engine charge entered the underwing air inlet as shown in figure 2(a). The engine and intercooler air exhausted through the outlets shown in figure 2(b). The oil cooler and engine charge air exhausted through the outlets indicated in figure 2(c). Several views of this configuration before being assembled are presented in figure 3.

The circular tapered plug flap in the engine cooling-air exit slot (fig. 2(b)) was moved fore and aft to regulate the engine air-flow rate, while flush-sliding and hinged-flap doors (figs. 2(b) and 2(c)) were used, respectively, to regulate the rate of air flow through the intercooler and oil-cooler cooling-air ducts. A clay constriction within the engine-charge-air duct(s) at a point near the exit(s) was used to regulate the charge-air flow.

Thin multiple-hole orifice plates, referred to herein as baffles, were inserted in the ducts to simulate the resistance of the various heat exchangers. The locations of these baffles are shown in figure 1. By covering a sufficient number of the orifices with cellulose tape, the total-pressure loss coefficient $\frac{\Delta P}{q_o}$ called for in the test specifications (table II) were obtained for each of the flow conditions investigated. No heat was added to simulate actual flow conditions.

The model with large and small beaver-tail fairings and with a wing-nacelle fillet is shown in figure 4. These modifications were made with modeling clay.

[redacted]

Configuration 2.- This configuration, shown in figures 5 and 6, incorporated changes to the lower lip of the upper duct inlet, underwing air inlet, and the engine charge, oil-cooler, and intercooler ducts of configuration 1. A sketch showing the revisions made to the leading edge and underwing air-inlet shapes along the nacelle center line is presented in figure 7. As a result of these modifications, the underwing air-inlet area was increased with a consequent reduction in inlet velocity for given flow rates. The engine charge-air duct outlet areas were retained; the ducts, however, were redesigned to permit the discharge air to flow parallel to the thrust line. In an effort to reduce the total-pressure losses, both the oil-cooler and intercooler cooling-air ducts were modified forward of the respective baffles, the locations of which are shown in figure 5. The contours of the intercooler cooling-air duct outlets were refaired (figs. 1 and 5) to discharge the air along the wing-nacelle juncture(s).

The pressure drop and the rate of flow through the various ducts were adjusted in the manner indicated for configuration 1.

TESTS AND TEST METHODS

Tests of the nacelle model and plain airfoil were made in the Langley two-dimensional low-turbulence tunnels. The tests included measurements of lift, drag, internal-duct losses and total-pressure surveys at various stations within the ducts at a Reynolds number of approximately 1.7×10^6. The air-flow characteristics over the nacelle at the air inlets and outlets and in the wing-nacelle junctures were determined by photographing the reaction of tufts. Additional drag measurements of configuration 2 were made at a Reynolds number of 4.3×10^6 for the simulated cruise condition at 40,000 feet.

For each simulated flow condition, the drag was measured at six model lift coefficients corresponding to calculated airplane lift coefficients submitted by the manufacturer. The nacelle drag coefficients obtained were based on the nacelle frontal area of 38.2 square inches, which is equivalent to 52 square feet full scale, and were determined from wake surveys by the methods described in reference 1.

In evaluating the influence of internal flow on the nacelle characteristics, the following assumptions were made to facilitate the tests. The validity of these assumptions is substantiated in reference 1. It was assumed that no appreciable changes in the

lift characteristics occur with change in internal flow for given angles of attack. The lift coefficients were measured, therefore, only at the beginning of the test and were corrected for tunnel-wall constriction effects by the methods described in reference 3. It was also assumed that the average loss in total pressure between the rear face of the baffles and the cooling-air outlets, about 1 percent of the free-stream dynamic pressure, is negligible. The total-pressure loss coefficients $\frac{\Delta P}{q_o}$ across the baffles were determined, therefore, by subtracting the average total pressure at the exits from that at the front face of the baffles.

RESULTS AND DISCUSSION

Aerodynamic force and internal pressure losses taken over a range of flow conditions including simulated cruise and climb operation requested by the manufacturer (table II) are presented in tabular and graphical form. The drag data, taken at a model lift coefficient of 0.845 which corresponds approximately to the cruise lift coefficient (C_L = 0.695) of the airplane, are summarized in table III where results for similar flight conditions of configurations 1 and 2 are given on the same line to facilitate comparison. The complete test results for configurations 1 and 2 are presented in tables IV to IX and X to XIII, respectively. The lift and drag characteristics of the plain airfoil, obtained at Reynolds numbers of 1.7×10^6 and 4.3×10^6, are presented in figure 8. The model was maintained in an aerodynamically smooth condition during all drag tests.

Preliminary measurements of model lift coefficient were made at a Reynolds number of 1.7×10^6 with the cooling-air outlets approximately half open and with the baffles removed from the ducts. The curves presented in figure 9 indicate that the differences between configurations 1 and 2 had no effect on the maximum lift coefficient, but the slope of the lift curve with configuration 2 was approximately 0.01 lower than that with configuration 1. It is seen by comparing figures 8 and 9 that the addition of the nacelle to the plain airfoil caused a 4-percent reduction in maximum lift at a Reynolds number of 1.7×10^6.

The results obtained from tests of configuration 1 with the baffles removed from the ducts (tables IV to VI) are presented in figure 10 as the variation of average total-pressure defect coefficient $\frac{\Delta H_e}{q_o}$ at the cooling-air outlets with flow coefficient $\frac{Q}{FV_o}$.

Since it had been assumed that the average loss in total pressure between the rear face of the baffles and the cooling-air outlets was negligible, the values of $\frac{\Delta H_e}{q_o}$, given in figure 10, were used for runs 4, 5, and 6 (tables VII to IX) as the equivalent of average total-pressure defect coefficients at the front face of the baffles. From these data, therefore, the measured $\frac{\Delta H_e}{q_o}$ for runs 4, 5, and 6 were subtracted to determine the values of the total-pressure loss coefficients $\frac{\Delta P}{q_o}$ across the baffles.

Drag.- Comparison of the drag characteristics between configurations 1 and 2 for the simulated cruise condition at altitudes of 10,000 and 40,000 feet and the simulated climb condition at 40,000 feet is presented in figures 11, 12, and 13, respectively.

It is seen from a reference to figures 11 and 12 that the increase in flow required for satisfactory engine cooling at the higher altitudes (one intercooler and one turbo) causes the total nacelle drag to increase; the internal nacelle drag increases more rapidly with flow rate than does the total nacelle drag. The external nacelle drag, therefore, decreases with increasing flow rate because of the improved alinement of the inlet lips at the higher values of inlet-velocity ratio.

A comparison of the external-nacelle-drag results for the simulated cruise conditions at 10,000 feet (fig. 11) and 40,000 feet (fig. 12) indicates that at the corresponding operating lift coefficients the external drag of configuration 1 is about 3 to 6 percent below that of configuration 2. The smaller internal nacelle drags of configuration 2 as compared with configuration 1 due to the decreases in duct losses more than compensate the slight increase in external nacelle drag.

For the simulated climb condition at 40,000 feet (fig. 13), the external nacelle drag of configuration 1 is shown to be unsatisfactory through the range of lift coefficients investigated. It was for this reason, in particular, that the model was modified. The total drag of the modified model, in general, (configuration 2) is lower than that of nacelle configuration 1 for all flight conditions investigated entirely because of the improvements made in the internal ducting system. At the simulated 40,000-foot climb condition, the external drag of nacelle configuration 2, corresponding to a lift coefficient of 0.912, was found to be approximately 52 percent less than that of configuration 1 due to increasing the stagger angle and lip radii of the air inlets.

[redacted]

It is to be noted that the pressure drop across the baffle simulating the engine for the runs indicated in figure 12 (cruise at 40,000 feet) was unobtainable with the required flow coefficient. Since the heating and propeller effects were not simulated, definite conclusions can not be drawn regarding the sufficiency of the available pressure drop. The present data indicate, however, that the cooling fan might be required for the 40,000-foot cruise condition and almost certainly will be required for the 40,000-foot climb condition.

It is pointed out in reference 4 that external nacelle drag tends to decrease with decreasing relative nacelle diameter until the nacelle diameter becomes equal to the wing thickness. In the case of the nacelles for the XB-36 airplane, not only are the differences in external nacelle drag, between configuration 2 of this paper and configuration 3 of reference 1, small for any of the three flow conditions investigated at the respective operating lift coefficients, but the ratio of wing thickness to nacelle diameter for the outboard nacelle is smaller than that for the inboard nacelle. Under these conditions, therefore, the drag results obtained from tests of outboard nacelle configuration 2 are less than expected on the basis of the inboard nacelle results. The external nacelle drags of the pusher-type nacelle (configuration 2) described in the present investigation are approximately one-third to one-half of those of conventional tractor nacelles (references 4 and 5) of equivalent ratio of wing thickness to nacelle diameter.

The effects of increased Reynolds number on nacelle drag for the simulated cruise condition at 40,000 feet (configuration 2) are shown in figure 14. The baffle adjustments and cooling-air-outlet areas were the same for runs 8 and 9. Since scale effect on pressure drop is not normally the same for the baffle as for the full-scale installation, no attempt was made to measure the total-pressure losses at the face of the baffles.

The external fairings added to configuration 1 are shown in figures 4(a) to 4(c). The effects of these modifications on nacelle drag were determined at an airplane lift coefficient of 0.695 for the flow conditions simulating cruise at 10,000 feet (one intercooler and one turbo). It was found that only small variations in external nacelle drag, within the limit of experimental accuracy, existed as a result of adding the beaver-tail-shape fairings and wing-nacelle fillets to configuration 1. In view of the probable weight increase entailed, these modifications were considered undesirable and the tests of this nature were discontinued.

[redacted]

Total-pressure defect in cooling-air ducts.- The variation of average total-pressure defect with chordwise position within the engine, intercooler and oil-cooler cooling-air ducts of configurations 1 and 2 are presented in figures 15(a) to 15(c), respectively. For these tests, the total-pressure measurements were made over a range of lift coefficients from 0.409 to 0.943 with the flow rates and pressure-drop coefficients adjusted to simulate climb at 40,000 feet.

The major differences in the average total-pressure defect through the engine cooling-air duct of configurations 1 and 2 occur at an airplane lift coefficient of 0.943. At this lift coefficient the losses at the front spar, cooling fan, and rear of the diffuser of configuration 2 are, respectively, about 17, 60, and 75 percent of those of configuration 1. These improvements in pressure recovery are attributed to increasing the stagger angle and lower lip radii of the leading-edge air inlet.

The improvement in the pressure recovery within the intercooler cooling-air ducts of configuration 2 as compared with configuration 1 (fig. 15(b)) between the front spar and baffle is due to the combination of refairing the ducts to reduce the velocity and to increasing the stagger angle and lower lip radii of the leading-edge air inlet. The differences in the total-pressure recoveries at the oil cooler (baffle) front face may not be as large as shown by figure 15(c) because of the differences in location of the baffles (figs. 2 and 5) and, hence, the position of measurement. Since the location of the baffle in the oil-cooler cooling-air duct of configuration 2 more nearly approximates that of the full-scale installation, the results for configuration 2 are considered applicable and are more favorable as compared with configuration 1 due to increasing the underwing air-inlet area, lip radii, and stagger angle and to refairing the entire duct up to the baffle.

Design considerations.- Moving-picture records of the behavior of tufts attached to the wing and nacelle were obtained with the flow rates and pressure drop coefficients adjusted to simulate the cruise condition at 40,000 feet (one intercooler and one turbo). These records (not shown) indicated that the discharging intercooler cooling air alleviated the stall condition in the wing-nacelle juncture, particularly at high angles of attack. It is thought, therefore, that for those flight conditions requiring single intercooler operation, some improvement in external drag may be realized by opening the auxiliary intercooler cooling-air outlet door so that the discharging air will flow into the wing-nacelle juncture. Propeller operation, as shown in reference 2, does not appear to

[redacted]

alleviate the stall condition at the trailing edge of the wing in the vicinity of the nacelle at high lift coefficients. For this reason, further reductions in nacelle drag with power on are not believed probable.

CONCLUSIONS

Two-dimensional wind-tunnel tests of two $\frac{1}{14}$-scale model configurations of an outboard nacelle for the XB-36 airplane were obtained, for the most part, at a Reynolds number of about 1.7×10^6 over a range of lift coefficients at three representative flow conditions. The results of these tests have indicated the following conclusions:

1. The total drag of nacelle configuration 2, in general, was lower than that of nacelle configuration 1 for all flight conditions investigated entirely because of the improvements made in the internal ducting system.

2. At the simulated 40,000-foot climb condition, the external drag of nacelle configuration 2, corresponding to a lift coefficient of 0.912, was approximately 52 percent less than that of configuration 1 due to increasing the stagger angle and lip radii of the air inlets.

3. The external drag coefficients of nacelle configuration 2 are approximately one-third to one-half of those of conventional tractor designs having the same ratio of wing thickness to nacelle diameter.

4. The cooling fan might be required for the 40,000-foot cruise condition and almost certainly will be required for the 40,000-foot climb condition.

Langley Memorial Aeronautical Laboratory
National Advisory Committee for Aeronautics
Langley Field, Va.

Robert J. Nuber
Aeronautical Engineer

Approved:
Clinton H. Dearborn
Chief of Full-Scale Research Division

CGB [redacted]

REFERENCES

1. Nuber, Robert J.: Development of Inboard Nacelle for the XB-36 Airplane. NACA RM No. L6J11, Army Air Forces, 1946.

2. Alexander, S. R. and Sivells, James C.: Tests of a $\frac{1}{14}$-Scale Powered Model of the XB-36 Airplane in the Langley 19-Foot Pressure Tunnel. I - Stalling Characteristics and Aileron Effectiveness of Several Wing and Flap Arrangements. NACA MR No. L5B23, 1945.

3. von Doenhoff, Albert E., and Abbott, Frank T., Jr.: The Langley Two-Dimensional Low-Turbulence Pressure Tunnel. NACA TN No. 1283, May 1947.

4. McHugh, James G.: Tests of Several Model Nacelle-Propeller Arrangements in Front of a Wing. NACA ACR, Sept. 1939.

5. Becker, John V.: High-Speed Tests of Radial-Engine Nacelles on a Thick Low-Drag Wing. NACA ACR, May 1942.

[redacted]

[redacted]

TABLE I

ORDINATES FOR THE NACA 63(420)-4(20.7)(approx.) AIRFOIL

[Stations and ordinates given in percent of airfoil chord]

Station	Upper surface	Lower surface
0	0.428	0.867
.312	1.283	1.723
.625	1.796	2.242
1.25	2.547	2.981
2.5	3.653	3.903
3.75	4.526	4.539
5.0	5.265	5.053
7.5	6.530	5.907
10	7.580	6.585
12	8.307	7.043
12.5	8.472	7.147
15	9.230	7.605
20	10.439	8.289
25	11.300	8.717
30	11.814	8.869
35	11.978	8.741
40	11.881	8.393
43	11.716	8.106
45	11.563	7.898
50	11.056	7.232
55	10.390	6.512
60	9.572	5.687
65	8.613	4.801
70	7.538	3.873
75	6.347	2.920
80	5.070	1.979
85	3.757	1.112
90	2.437	.415
95	1.197	.018
100	0	0
L.E. radius: 3.360		

[redacted]

NATIONAL ADVISORY
COMMITTEE FOR AERONAUTICS

TABLE II.- TEST SPECIFICATIONS FOR $\frac{1}{14}$-SCALE MODEL OF XB-36 OUTBOARD NACELLE

[Except as noted, all runs were made in the Langley two-dimensional low-turbulence tunnel at a Reynolds number of approximately 1.68×10^6; when single intercooler or engine-charge-air operation was required the right hand exits were sealed; flap and flush type doors were used respectively on the oil-cooler and intercooler cooling-air outlets]

[redacted]

Run		Engine cooling air		Oil cooler cooling air		Intercooler cooling air		Engine charge air	Altitude (ft)	Flight condition	C_L	Remarks
Configuration 1	Configuration 2	$\frac{Q}{FV_o}$	$\frac{\Delta P}{q_o}$	$\frac{Q}{FV_o}$	$\frac{\Delta P}{q_o}$	$\frac{Q}{FV_o}$	$\frac{\Delta P}{q_o}$	$\frac{Q}{FV_o}$				
1		0.0252	-----	0.0068	-----	0.0010	-----	0.0030	10,000	Cruise	0.685	No baffles
2		.0370	-----	.0130	-----	.0069	-----	.0059	40,000	Cruise	.667	
[a]3		.0450	-----	.0176	-----	.0165	-----	.0113	40,000	Climb	.912	
4	7	.0252	0.284	.0068	0.105	.0010	0.017	.0030	10,000	Cruise	.685	Effects of beaver-tail fairings and fillets on drag determined for configuration 1 at $C_L = 0.695$
5	8	.0370	.730	.0130	.397	.0069	.360	.0059	40,000	Cruise	.667	Behavior of tufts on nacelle and wing were photographed
9	9	.0370	(c)	.0130	(c)	.0069	(c)	.0059	40,000	Cruise	.667	$R = 4.28 \times 10^6$, TDT[b]
[a]6	[a]10	.0450	max	.0176	.667	.0165	.527	.0113	40,000	Climb	.912	Total pressure recoveries measured in cooling-air ducts

[a]Both intercooler and engine charge-air ducts open.
[b]Two-dimensional low-turbulence pressure tunnel.
[c]Same baffle setting as run 8.

NATIONAL ADVISORY
COMMITTEE FOR AERONAUTICS

TABLE III.- TEST RECORD FOR $\frac{1}{14}$-SCALE MODEL OF XB-36 OUTBOARD NACELLE

[Results presented for $C_L = 0.695$]

Configuration 1											Configuration 2										
Run	Figure	Table	Engine cooling air		Oil cooler cooling air		Intercooler cooling air		Engine charge air	C_{D_F} (a)	C_{D_P} (a)	Run	Figure	Table	Engine cooling air		Oil cooler cooling air		Intercooler cooling air		Engine charge air	C_{D_F} (a)	C_{D_P} (a)
			$\frac{Q}{FV_o}$	$\frac{\Delta P}{q_o}$	$\frac{Q}{FV_o}$	$\frac{\Delta P}{q_o}$	$\frac{Q}{FV_o}$	$\frac{\Delta P}{q_o}$	$\frac{Q}{FV_o}$						$\frac{Q}{FV_o}$	$\frac{\Delta P}{q_o}$	$\frac{Q}{FV_o}$	$\frac{\Delta P}{q_o}$	$\frac{Q}{FV_o}$	$\frac{\Delta P}{q_o}$	$\frac{Q}{FV_o}$		
1	10	IV	0.0237	-----	0.0070	-----	0.0011	-----	0.0032	(b)	(b)												
2	10	V	.0369	-----	.0129	-----	.0068	-----	.0061	(b)	(b)												
3	10	VI	.0472	-----	.0180	-----	.0160	-----	.0113	(b)	(b)												
4	11	VII	.0244	0.328	.0067	0.101	.0011	0.012	.0030	0.0492	0.0360	7	11	X	0.0261	0.300	0.0065	0.117	0.0010	0.009	0.0029	0.0492	0.0376
5	12	VIII	.0379	.607	.0135	.392	.0068	.354	.0062	.0789	.0239	8	12 and 14	XI	.0354	.639	.0133	.385	.0070	.376	.0061	.0728	.0262
												9	14	XII	.0359	(b)	.0130	(b)	.0071	(b)	.0058	.0731	.0260
6	13	IX	.0485	.552	.0181	.672	.0165	.492	.0110	.1737	.0690	10	13	XIII	.0464	.514	.0181	.687	.0176	.519	.0111	.0998	.0221

[a]Obtained from faired curve plotted against C_L.
[b]Not measured.

[redacted]

NATIONAL ADVISORY
COMMITTEE FOR AERONAUTICS

[redacted]

TABLE IV -- RESULTS OF COOLING TESTS OF $\frac{1}{14}$-SCALE MODEL OF XB-36 OUTBOARD NACELLE WITH LEADING-EDGE AIR INLETS

RUN 1

COMPLETE MODEL CONFIGURATION 1						LOWER DUCT INLET										
AIRPLANE		C_l	C_{D_i}	C_{D_P}	C_{D_P}	$\frac{V_n}{V_o}$	OIL-COOLER					LEFT-HAND ENGINE CHARGE-AIR DUCT				
							$\frac{\Delta H}{q_o}$ EXIT		$\frac{\Delta P}{q_o}$	$\frac{q}{FV_o}$	C_{D_i}	$\frac{\Delta H}{q_o}$ EXIT		$\frac{\Delta P}{q_o}$	$\frac{q}{FV_o}$	C_{D_i}
α	C_L		INTERNAL	TOTAL	EXTERNAL		NO BAFFLE	BAFFLE				NO BAFFLE	BAFFLE			
3.0	0.409	0.526				0.35	0.110	—	—	0.0073	—	0.116	—	—	0.0033	—
5.0	.589	.726				.34	.109	—	—	.0071	—	.120	—	—	.0032	—
6.2	.695	.845				.33	.112	—	—	.0070	—	.114	—	—	.0032	—
7.0	.767	.924				.33	.117	—	—	.0069	—	.116	—	—	.0032	—
8.2	.875	1.045				.32	.129	—	—	.0067	—	.111	—	—	.0032	—
9.0	.943	1.121				.32	.142	—	—	.0065	—	.113	—	—	.0032	—

UPPER DUCT INLET											
C_l	$\frac{V_n}{V_o}$	ENGINE AIR DUCT					LEFT-HAND INTERCOOLER DUCT				
		$\frac{\Delta H}{q_o}$ EXIT		$\frac{\Delta P}{q_o}$	$\frac{q}{FV_o}$	C_{D_i}	$\frac{\Delta H}{q_o}$ EXIT		$\frac{\Delta P}{q_o}$	$\frac{q}{FV_o}$	C_{D_i}
		NO BAFFLE	BAFFLE				NO BAFFLE	BAFFLE			
0.526	0.39	0.087	—	—	0.0256	—	0.029	—	—	0.0011	—
.726	.39	.086	—	—	.0257	—	.028	—	—	.0011	—
.845	.39	.096	—	—	.0257	—	.030	—	—	.0011	—
.924	.39	.118	—	—	.0257	—	.036	—	—	.0011	—
1.045	.39	.165	—	—	.0256	—	.054	—	—	.0012	—
1.121	.39	.239	—	—	.0257	—	.079	—	—	.0012	—

[redacted]

[redacted]AL

TABLE V -- RESULTS OF COOLING TESTS OF $\frac{1}{14}$-SCALE MODEL OF XB-36 OUTBOARD NACELLE WITH LEADING-EDGE AIR INLETS

RUN 3

COMPLETE MODEL CONFIGURATION 1						LOWER DUCT INLET											
AIRPLANE		C_l	C_{D_i}	C_{D_p}	C_{D_p}	$\frac{V}{V_o}$	OIL-COOLER					LEFT-HAND ENGINE CHARGE-AIR DUCT					
							$\frac{\Delta H}{q_o}$ EXIT		$\frac{\Delta p}{q_o}$	$\frac{Q}{FV_o}$	C_{D_i}	$\frac{\Delta H}{q_o}$ EXIT		$\frac{\Delta p}{q_o}$	$\frac{Q}{FV_o}$	C_{D_i}
α	C_L		INTERNAL	TOTAL	EXTERNAL		NO BAFFLE	BAFFLE				NO BAFFLE	BAFFLE			
3.0	0.409	0.526				0.65	0.272	—	—	0.0136	—	0.100	—	—	0.0062	—
5.0	.589	.726				.63	.281	—	—	.0131	—	.090	—	—	.0062	—
6.2	.695	.845				.62	.280	—	—	.0129	—	.092	—	—	.0061	—
7.0	.767	.924				.61	.282	—	—	.0126	—	.096	—	—	.0060	—
8.2	.875	1.045				.59	.296	—	—	.0122	—	.102	—	—	.0059	—
9.0	.943	1.121				.58	.318	—	—	.0118	—	.114	—	—	.0059	—

UPPER DUCT INLET												
C_l	$\frac{V}{V_o}$	ENGINE AIR DUCT					LEFT-HAND INTERCOOLER DUCT					
		$\frac{\Delta H}{q_o}$ EXIT		$\frac{\Delta p}{q_o}$	$\frac{Q}{FV_o}$	C_{D_i}	$\frac{\Delta H}{q_o}$ EXIT		$\frac{\Delta p}{q_o}$	$\frac{Q}{FV_o}$	C_{D_i}
		NO BAFFLE	BAFFLE				NO BAFFLE	BAFFLE			
0.526	0.63	0.127	—	—	0.0367	—	0.204	—	—	0.0066	—
.726	.64	.134	—	—	.0370	—	.235	—	—	.0068	—
.845	.64	.142	—	—	.0369	—	.254	—	—	.0068	—
.924	.62	.179	—	—	.0361	—	.301	—	—	.0067	—
1.045	.62	.235	—	—	.0361	—	.377	—	—	.0068	—
1.121	.63	.298	—	—	.0365	—	.453	—	—	.0067	—

[redacted]

NATIONAL ADVISORY COMMITTEE FOR AERONAUTICS

TABLE VI -- RESULTS OF COOLING TESTS OF $\frac{1}{14}$-SCALE MODEL OF XB-30 OUTBOARD NACELLE WITH LEADING-EDGE AIR INLETS

RUN 3

COMPLETE MODEL CONFIGURATION 1						LOWER DUCT INLET											
AIRPLANE		C_L	C_{D_i}	C_{D_F}	C_{D_P}	$\frac{V_n}{V_o}$	OIL-COOLER					ENGINE CHARGE-AIR DUCTS					
							$\frac{\Delta H}{q_o}$ EXIT		$\frac{\Delta P}{q_o}$	$\frac{Q}{FV_o}$	C_{D_i}	$\frac{\Delta H}{q_o}$ EXIT		$\frac{\Delta P}{q_o}$	$\frac{Q}{FV_o}$	C_{D_i}
α	C_L		INTERNAL	TOTAL	EXTERNAL		NO BAFFLE	BAFFLE				NO BAFFLE	BAFFLE			
3.0	0.409	0.526				1.01	0.476	—	—	0.0192	—	0.187	—	—	0.0117	—
5.0	.589	.726				.96	.462	—	—	.0181	—	.182	—	—	.0114	—
6.2	.695	.845				.96	.465	—	—	.0180	—	.184	—	—	.0113	—
7.0	.767	.924				.94	.474	—	—	.0176	—	.182	—	—	.0112	—
8.2	.875	1.045				.91	.480	—	—	.0169	—	.181	—	—	.0110	—
9.0	.943	1.121				.88	.502	—	—	.0162	—	.195	—	—	.0108	—

UPPER DUCT INLET												
C_l	$\frac{V_n}{V_o}$	ENGINE AIR DUCT					INTERCOOLER DUCTS					
		$\frac{\Delta H}{q_o}$ EXIT		$\frac{\Delta P}{q_o}$	$\frac{Q}{FV_o}$	C_{D_i}	$\frac{\Delta H}{q_o}$ EXIT		$\frac{\Delta P}{q_o}$	$\frac{Q}{FV_o}$	C_{D_i}
		NO BAFFLE	BAFFLE				NO BAFFLE	BAFFLE			
0.526	0.92	0.165	—	—	0.0475	—	0.338	—	—	0.0156	—
.726	.92	.166	—	—	.0475	—	.348	—	—	.0160	—
.845	.92	.171	—	—	.0472	—	.358	—	—	.0160	—
.924	.92	.186	—	—	.0469	—	.377	—	—	.0161	—
1.045	.86	.331	—	—	.0426	—	.445	—	—	.0163	—
1.121	.84	.437	—	—	.0418	—	.483	—	—	.0161	—

TABLE VII .- RESULTS OF COOLING AND DRAG TESTS OF $\frac{1}{14}$-SCALE MODEL OF XB-36 OUTBOARD NACELLE WITH LEADING-EDGE AIR INLETS

RUN 4

COMPLETE MODEL CONFIGURATION 1						LOWER DUCT INLET										
							OIL-COOLER					LEFT-HAND ENGINE CHARGE-AIR DUCT				
AIRPLANE		C_L	C_{D_i}	C_{D_F}	C_{D_P}	$\frac{V_n}{V_o}$	$\frac{\Delta H}{q_o}$ EXIT		$\frac{\Delta P}{q_o}$	$\frac{Q}{FV_o}$	C_{D_i}	$\frac{\Delta H}{q_o}$ EXIT		$\frac{\Delta P}{q_o}$	$\frac{Q}{FV_o}$	C_{D_i}
α	τ_L		INTERNAL	TOTAL	EXTERNAL		NO BAFFLE	BAFFLE				NO BAFFLE	BAFFLE			
3.0	0.409	0.526	0.0129	0.0505	0.0376	0.33	0.104	0.221	0.117	0.0070	0.0016	0.034	——	——	0.0031	0.0001
5.0	.589	.726	.0129	.0468	.0339	.32	.101	.206	.105	.0068	.0015	.036	——	——	.0031	.0001
6.2	.695	.845	.0130	.0473	.0343	.32	.104	.205	.101	.0067	.0014	.042	——	——	.0030	.0001
7.0	.767	.924	.0134	.0535	.0401	.31	.110	.201	.091	.0066	.0014	.042	——	——	.0030	.0001
8.2	.875	1.045	.0147	.1040	.0893	.31	.124	.189	.065	.0065	.0013	.041	——	——	.0030	.0001
9.0	.943	1.121	.0177	——	——	.30	.135	.200	.065	.0063	.0013	.040	——	——	.0030	.0001

UPPER DUCT INLET											
		ENGINE AIR DUCT					LEFT-HAND INTERCOOLER DUCT				
C_L	$\frac{V_n}{V_o}$	$\frac{\Delta H}{q_o}$ EXIT		$\frac{\Delta P}{q_o}$	$\frac{Q}{FV_o}$	C_{D_i}	$\frac{\Delta H}{q_o}$ EXIT		$\frac{\Delta P}{q_o}$	$\frac{Q}{FV_o}$	C_{D_i}
		NO BAFFLE	BAFFLE				NO BAFFLE	BAFFLE			
0.526	0.37	0.078	0.411	0.333	0.0242	0.0113	0.029	0.040	0.011	0.0011	0.0000
.726	.37	.078	.414	.336	.0243	.0113	.028	.043	.013	.0011	.0000
.845	.37	.091	.419	.328	.0244	.0116	.030	.042	.012	.0011	.0001
.924	.37	.108	.430	.322	.0243	.0119	.036	.047	.011	.0011	.0001
1.045	.37	.158	.475	.317	.0243	.0113	.047	.059	.012	.0011	.0001
1.121	.37	.236	.556	.320	.0245	.0163	.079	.082	.003	.0012	.0001

[redacted]

NATIONAL ADVISORY COMMITTEE FOR AERONAUTICS

TABLE VIII.- RESULTS OF COOLING AND DRAG TESTS OF $\frac{1}{14}$-SCALE MODEL OF XB-86 OUTBOARD NACELLE WITH LEADING-EDGE AIR INLETS

RUN 5

COMPLETE MODEL CONFIGURATION 1.						LOWER DUCT INLET										
							OIL-COOLER					LEFT-HAND ENGINE CHARGE-AIR DUCT				
AIRPLANE		C_L	C_{D_i}	C_{D_P}	C_{D_P}	$\frac{V_n}{V_o}$	$\frac{\Delta H}{q_o}$ EXIT		$\frac{\Delta p}{q_o}$	$\frac{Q}{FV_o}$	C_{D_i}	$\frac{\Delta H}{q_o}$ EXIT		$\frac{\Delta p}{q_o}$	$\frac{Q}{FV_o}$	C_{D_i}
α	C_L		INTERNAL	TOTAL	EXTERNAL		NO BAFFLE	BAFFLE				NO BAFFLE	BAFFLE			
3.0	0.409	0.526	0.0550	0.0815	0.0265	0.68	0.292	0.734	0.442	0.0142	0.0137	0.127	——	——	0.0065	0.0008
5.0	.589	.726	.0548	.0761	.0213	.66	.303	.709	.406	.0138	.0127	.120	——	——	.0064	.0008
6.2	.695	.845	.0551	.0801	.0250	.64	.300	.692	.392	.0135	.0120	.118	——	——	.0062	.0008
7.0	.767	.924	.0547	.0834	.0287	.63	.305	.682	.377	.0133	.0116	.122	——	——	.0061	.0008
8.2	.875	1.045	.0607	.1263	.0656	.62	.325	.667	.342	.0130	.0110	.129	——	——	.0061	.0008
9.0	.943	1.121	.0699	——	——	.61	.357	.665	.308	.0128	.0108	.139	——	——	.0060	.0009

UPPER DUCT INLET											
		ENGINE AIR DUCT					LEFT-HAND INTERCOOLER DUCT				
C_l	$\frac{V_n}{V_o}$	$\frac{\Delta H}{q_o}$ EXIT		$\frac{\Delta p}{q_o}$	$\frac{Q}{FV_o}$	C_{D_i}	$\frac{\Delta H}{q_o}$ EXIT		$\frac{\Delta p}{q_o}$	$\frac{Q}{FV_o}$	C_{D_i}
		NO BAFFLE	BAFFLE				NO BAFFLE	BAFFLE			
0.526	0.65	0.131	0.734	0.603	0.0381	0.0368	0.204	0.562	0.358	0.0066	0.0045
.726	.65	.135	.746	.611	.0377	.0373	.235	.579	.344	.0068	.0048
.845	.65	.144	.751	.607	.0379	.0380	.254	.608	.354	.0068	.0051
.924	.62	.179	.771	.592	.0361	.0377	.312	.631	.319	.0069	.0054
1.045	.64	.246	.829	.583	.0372	.0437	.372	.697	.325	.0067	.0060
1.121	.66	.330	.896	.566	.0385	.0522	.453	.768	.315	.0067	.0069

TABLE IX - RESULTS OF COOLING AND DRAG TESTS OF $\frac{1}{14}$-SCALE MODEL OF XB-38 OUTBOARD NACELLE WITH LEADING-EDGE AIR INLETS

RUN 8

COMPLETE MODEL CONFIGURATION 1						LOWER DUCT INLET										
							OIL-COOLER					ENGINE CHARGE-AIR DUCTS				
AIRPLANE		C_l	C_{D_i}	C_{D_F}	C_{D_P}	$\frac{V_n}{V_o}$	$\frac{\Delta H}{q_o}$ EXIT		$\frac{\Delta p}{q_o}$	$\frac{Q}{FV_o}$	C_{D_i}	$\frac{\Delta H}{q_o}$ EXIT		$\frac{\Delta p}{q_o}$	$\frac{Q}{FV_o}$	C_{D_i}
α	C_L		INTERNAL	TOTAL	EXTERNAL		NO BAFFLE	BAFFLE				NO BAFFLE	BAFFLE			
3.0	0.409	0.526	0.1031	0.1692	0.0661	0.99	0.476	1.181	0.705	0.0192	0.0383	0.142	----	----	0.0113	0.0017
5.0	.589	.726	.1036	.1757	.0721	.96	.473	1.160	.687	.0184	.0367	.137	----	----	.0111	.0016
6.2	.695	.845	.1046	.1690	.0644	.95	.469	1.141	.672	.0181	.0362	.144	----	----	.0110	.0017
7.0	.767	.924	.1059	.1846	.0787	.95	.490	1.126	.636	.0180	.0360	.141	----	----	.0110	.0016
8.2	.875	1.045	.1117	.1913	.0796	.93	.515	1.105	.590	.0177	.0353	.147	----	----	.0107	.0016
9.0	.943	1.121	.1222	.2523	.1301	.91	.552	1.092	.540	.0173	.0346	.164	----	----	.0105	.0018

UPPER DUCT INLET											
		ENGINE AIR DUCT					INTERCOOLER DUCTS				
C_l	$\frac{V_n}{V_o}$	$\frac{\Delta H}{q_o}$ EXIT		$\frac{\Delta p}{q_o}$	$\frac{Q}{FV_o}$	C_{D_i}	$\frac{\Delta H}{q_o}$ EXIT		$\frac{\Delta p}{q_o}$	$\frac{Q}{FV_o}$	C_{D_i}
		NO BAFFLE	BAFFLE				NO BAFFLE	BAFFLE			
0.526	0.94	0.167	0.705	0.538	0.0480	0.0437	0.403	0.872	0.469	0.0164	0.0211
.726	.94	.167	.715	.548	.0484	.0449	.379	.884	.505	.0165	.0220
.845	.94	.174	.726	.552	.0485	.0461	.404	.896	.492	.0165	.0223
.924	.94	.187	.741	.554	.0480	.0469	.390	.909	.519	.0165	.0230
1.045	.90	.403	.808	.405	.0453	.0509	.449	.952	.503	.0164	.0255
1.121	.88	.541	.871	.330	.0440	.0565	.483	.997	.514	.0165	.0311

TABLE X .- RESULTS OF COOLING AND DRAG TESTS OF $\frac{1}{14}$-SCALE MODEL OF XB-35 OUTBOARD NACELLE WITH LEADING-EDGE AIR INLETS

RUN 7

COMPLETE MODEL CONFIGURATION 2						LOWER DUCT INLET										
							OIL-COOLER					LEFT-HAND ENGINE CHARGE-AIR DUCT				
AIRPLANE		C_l	C_{D_i}	C_{D_F}	C_{D_P}	$\frac{V_n}{V_o}$	$\frac{\Delta H}{q_o}$		$\frac{\Delta P}{q_o}$	$\frac{Q}{FV_o}$	C_{D_i}	$\frac{\Delta H}{q_o}$		$\frac{\Delta P}{q_o}$	$\frac{Q}{FV_o}$	C_{D_i}
α	C_L		INTERNAL	TOTAL	EXTERNAL		BAFFLE	EXIT				BAFFLE	EXIT			
3.0	0.409	0.526	0.0116	0.0398	0.0282	0.28	0.101	0.223	0.122	0.0067	0.0016	——	0.094	——	0.0029	0.0003
5.0	.589	.726	.0114	.0447	.0333	.28	.050	.166	.116	.0066	.0012	——	.027	——	.0029	.0001
6.2	.695	.845	.0116	.0492	.0376	.28	.044	.161	.117	.0065	.0011	——	.029	——	.0029	.0001
7.0	.767	.924	.0118	.0558	.0440	.27	.045	.151	.106	.0065	.0010	——	.035	——	.0029	.0001
8.2	.875	1.045	.0130	.0896	.0766	.27	.046	.148	.102	.0063	.0010	——	.039	——	.0029	.0001
9.0	.943	1.121	.0158	——	——	.27	.048	.147	.099	.0063	.0010	——	.036	——	.0029	.0001

UPPER DUCT INLET										
		ENGINE AIR DUCT					LEFT-HAND INTERCOOLER DUCT				
C_l	$\frac{V_n}{V_o}$	$\frac{\Delta H}{q_o}$		$\frac{\Delta P}{q_o}$	$\frac{Q}{FV_o}$	C_{D_i}	$\frac{\Delta H}{q_o}$		$\frac{\Delta P}{q_o}$	$\frac{Q}{FV_o}$	C_{D_i}
		BAFFLE	EXIT				BAFFLE	EXIT			
0.526	0.38	0.053	0.349	0.296	0.0259	0.0100	0.012	0.021	0.009	0.0010	0.0000
.726	.38	.055	.353	.298	.0260	.0102	.013	.022	.009	.0010	.0000
.845	.38	.059	.359	.300	.0261	.0104	.015	.025	.009	.0010	.0000
.924	.39	.066	.368	.302	.0263	.0108	.017	.023	.006	.0010	.0000
1.045	.39	.096	.400	.304	.0266	.0120	.023	.034	.011	.0011	.0000
1.121	.40	.145	.475	.330	.0269	.0148	.039	.046	.008	.0011	.0000

TABLE XI .- RESULTS OF COOLING AND DRAG TESTS OF $\frac{1}{14}$-SCALE MODEL OF XB-36 OUTBOARD NACELLE WITH LEADING-EDGE AIR INLETS

RUN 8

COMPLETE MODEL CONFIGURATION 2						LOWER DUCT INLET										
							OIL-COOLER					LEFT-HAND ENGINE CHARGE-AIR DUCT				
AIRPLANE		C_l	C_{D_i}	C_{D_F}	C_{D_P}	$\frac{V_n}{V_o}$	$\frac{\Delta H}{q_o}$		$\frac{\Delta P}{q_o}$	$\frac{Q}{FV_o}$	C_{D_i}	$\frac{\Delta H}{q_o}$		$\frac{\Delta P}{q_o}$	$\frac{Q}{FV_o}$	C_{D_i}
α	C_L		INTERNAL	TOTAL	EXTERNAL		BAFFLE	EXIT				BAFFLE	EXIT			
3.0	0.409	0.526	0.0456	0.0695	0.0239	0.59	0.137	0.568	0.431	0.0138	0.0094	——	0.039	——	0.0062	0.0002
5.0	.589	.726	.0459	.0695	.0236	.58	.135	.530	.395	.0135	.0085	——	.045	——	.0061	.0003
6.2	.695	.845	.0467	.0725	.0258	.57	.131	.516	.385	.0133	.0081	——	.042	——	.0061	.0003
7.0	.767	.924	.0473	.0778	.0305	.56	.130	.508	.378	.0132	.0079	——	.041	——	.0061	.0002
8.2	.875	1.045	.0487	.0984	.0497	.55	.128	.493	.365	.0129	.0074	——	.041	——	.0060	.0002
9.0	.943	1.121	.0540	——	——	.55	.129	.486	.357	.0127	.0072	——	.044	——	.0060	.0003

UPPER DUCT INLET											
		ENGINE AIR DUCT					LEFT-HAND INTERCOOLER DUCT				
C_l	$\frac{V_n}{V_o}$	$\frac{\Delta H}{q_o}$		$\frac{\Delta P}{q_o}$	$\frac{Q}{FV_o}$	C_{D_i}	$\frac{\Delta H}{q_o}$		$\frac{\Delta P}{q_o}$	$\frac{Q}{FV_o}$	C_{D_i}
		BAFFLE	EXIT				BAFFLE	EXIT			
0.526	0.58	0.088	0.716	0.628	0.0344	0.0320	0.166	0.512	0.346	0.0069	0.0042
.726	.59	.090	.722	.632	.0350	.0330	.165	.527	.362	.0070	.0044
.845	.60	.093	.732	.639	.0354	.0341	.161	.537	.376	.0070	.0045
.924	.60	.092	.738	.646	.0357	.0348	.171	.546	.375	.0070	.0046
1.045	.61	.115	.756	.641	.0361	.0365	.180	.562	.382	.0070	.0048
1.121	.63	.147	.805	.658	.0374	.0418	.269	.582	.313	.0070	.0050

NATIONAL ADVISORY COMMITTEE FOR AERONAUTICS

TABLE XII .- RESULTS OF COOLING AND DRAG TESTS OF $\frac{1}{14}$-SCALE MODEL OF XB-36 OUTBOARD NACELLE WITH LEADING-EDGE AIR INLETS

RUN 9 $R = 4.28 \times 10^6$ (TOT)

COMPLETE MODEL CONFIGURATION 2						LOWER DUCT INLET											
							OIL-COOLER					LEFT-HAND ENGINE CHARGE-AIR DUCT					
AIRPLANE		C_l	C_{D_i}	C_{D_F}	C_{D_P}	$\frac{V_n}{V_o}$	$\frac{\Delta H}{q_o}$		$\frac{\Delta p}{q_o}$	$\frac{q}{FV_o}$	C_{D_i}	$\frac{\Delta H}{q_o}$		$\frac{\Delta p}{q_o}$	$\frac{q}{FV_o}$	C_{D_i}	
α	C_L		INTERNAL	TOTAL	EXTERNAL		BAFFLE	EXIT				BAFFLE	EXIT				
3.0	0.409	0.526	0.0465	0.0730	0.0265	0.57	NOT MEASURED	0.535	—	0.0134	0.0086	—	0.015	—	0.0059	0.0001	
5.0	.589	.726	.0469	.0729	.0260	.56		.498	—	.0132	.0077	—	.019	—	.0059	.0001	
6.2	.695	.845	.0475	.0727	.0252	.55		.487	—	.0130	.0074	—	.019	—	.0058	.0001	
7.0	.767	.924	.0475	.0769	.0294	.55		.477	—	.0128	.0071	—	.019	—	.0058	.0001	
8.2	.875	1.045	.0492	.0977	.0485	.54		.469	—	.0126	.0068	—	.018	—	.0058	.0001	
9.0	.943	1.121	.0519	—	—	.53		.466	—	.0124	.0067	—	.021	—	.0058	.0001	

UPPER DUCT INLET											
		ENGINE AIR DUCT					LEFT-HAND INTERCOOLER DUCT				
C_l	$\frac{V_n}{V_o}$	$\frac{\Delta H}{q_o}$		$\frac{\Delta p}{q_o}$	$\frac{q}{FV_o}$	C_{D_i}	$\frac{\Delta H}{q_o}$		$\frac{\Delta p}{q_o}$	$\frac{q}{FV_o}$	C_{D_i}
		BAFFLE	EXIT				BAFFLE	EXIT			
0.526	0.59	NOT MEASURED	0.739	—	0.0346	0.0337	NOT MEASURED	0.517	—	0.0069	0.0042
.726	.60		.740	—	.0356	.0348		.535	—	.0070	.0045
.845	.61		.746	—	.0359	.0355		.548	—	.0071	.0046
.924	.61		.747	—	.0359	.0356		.563	—	.0071	.0049
1.045	.62		.761	—	.0363	.0370		.597	—	.0073	.0053
1.121	.62		.794	—	.0365	.0398		.602	—	.0073	.0054

TABLE XIII - RESULTS OF COOLING AND DRAG TESTS OF $\frac{1}{14}$-SCALE MODEL OF XB-36 OUTBOARD NACELLE
RUN 10
WITH LEADING-EDGE AIR INLETS

COMPLETE MODEL CONFIGURATION 3.						LOWER DUCT INLET										
							OIL-COOLER					ENGINE CHARGE-AIR DUCTS				
AIRPLANE		C_l	C_{D_i}	C_{D_F}	C_{D_P}	$\frac{V_n}{V_o}$	$\frac{\Delta H}{q_o}$		$\frac{\Delta p}{q_o}$	$\frac{Q}{FV_o}$	C_{D_i}	$\frac{\Delta H}{q_o}$		$\frac{\Delta p}{q_o}$	$\frac{Q}{FV_o}$	C_{D_i}
α	C_L		INTERNAL	TOTAL	EXTERNAL		BAFFLE	EXIT				BAFFLE	EXIT			
3.0	0.409	0.526	0.0793	0.0999	0.0206	0.89	0.119	0.870	0.751	0.0189	0.0242	—	0.085	—	0.0114	0.0010
5.0	.589	.726	.0774	.0991	.0217	.87	.126	.838	.712	.0183	.0219	—	.083	—	.0112	.0009
6.2	.695	.845	.0766	.0987	.0221	.86	.129	.816	.687	.0181	.0206	—	.090	—	.0111	.0010
7.0	.767	.924	.0772	.0996	.0224	.84	.134	.798	.664	.0176	.0194	—	.089	—	.0110	.0010
8.2	.875	1.045	.0797	.1158	.0361	.83	.150	.781	.631	.0174	.0185	—	.102	—	.0108	.0011
9.0	.943	1.121	.0855	.1765	.0910	.81	.167	.774	.607	.0169	.0177	—	.123	—	.0107	.0013

UPPER DUCT INLET										
		ENGINE AIR DUCT					INTERCOOLER DUCTS				
C_l	$\frac{V_R}{V_o}$	$\frac{\Delta H}{q_o}$		$\frac{\Delta p}{q_o}$	$\frac{Q}{FV_o}$	C_{D_i}	$\frac{\Delta H}{q_o}$		$\frac{\Delta p}{q_o}$	$\frac{Q}{FV_o}$	C_{D_i}
		BAFFLE	EXIT				BAFFLE	EXIT			
0.526	0.91	0.152	0.668	0.516	0.0470	0.0399	0.192	0.691	0.499	0.0171	0.0152
.726	.91	.151	.665	.514	.0468	.0393	.199	.713	.514	.0175	.0162
.845	.91	.152	.666	.514	.0464	.0393	.208	.727	.519	.0176	.0167
.924	.90	.156	.679	.523	.0463	.0402	.214	.751	.537	.0176	.0176
1.045	.91	.169	.696	.527	.0466	.0418	.248	.793	.545	.0178	.0194
1.121	.87	.303	.792	.489	.0438	.0476	.273	.827	.554	.0173	.0202

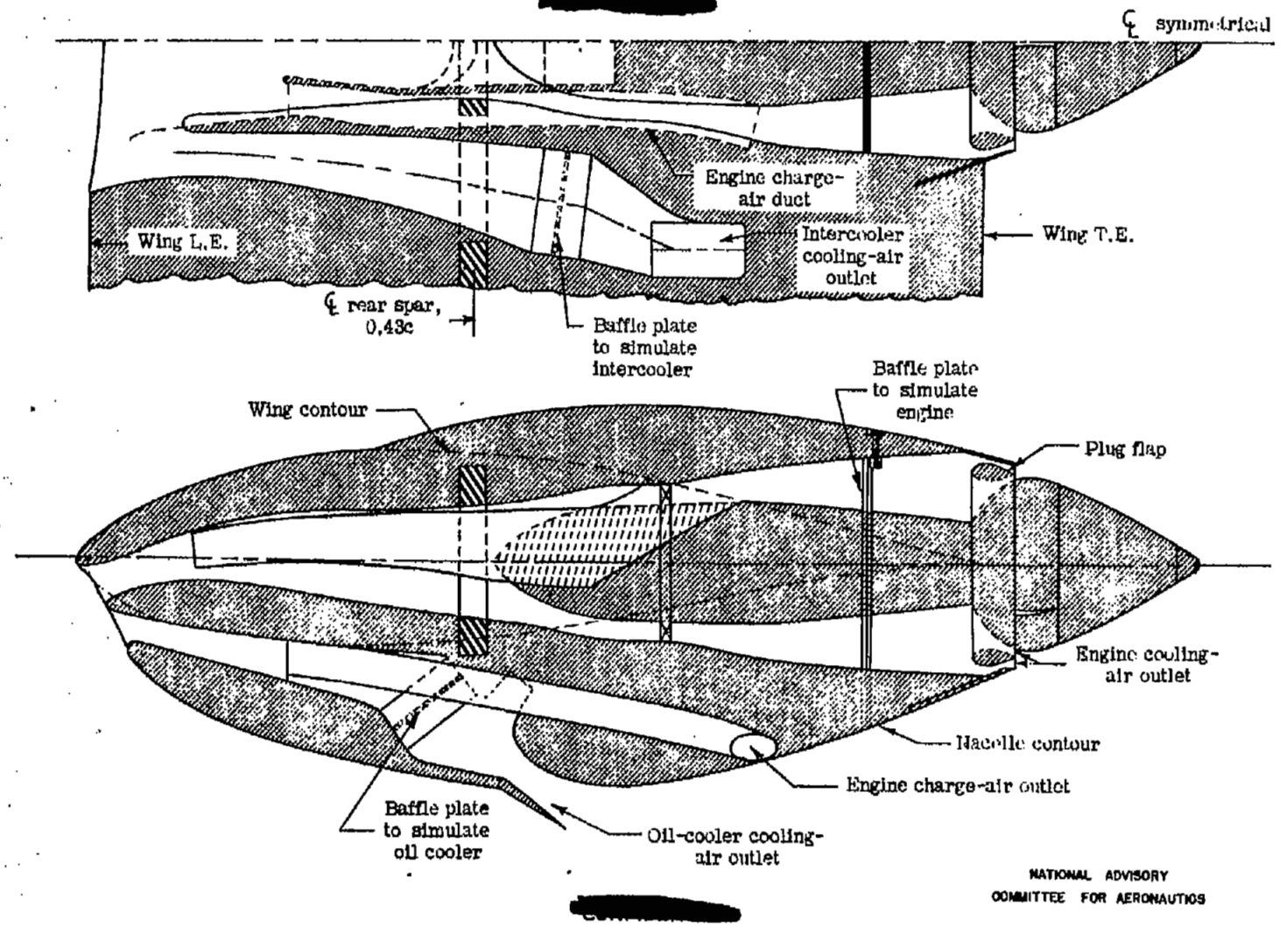

Figure 1.- General arrangement of $\frac{1}{14}$-scale model of XB-36 outboard nacelle; configuration 1.

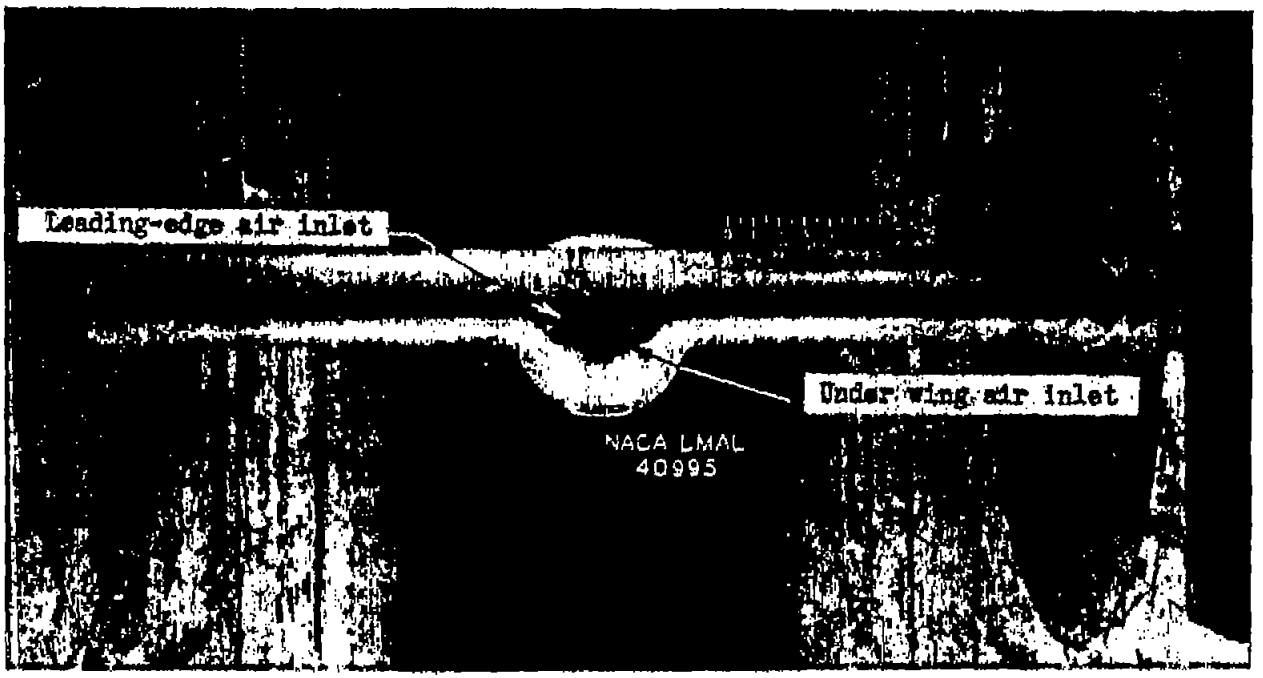

(a) Front view showing air inlets.

Figure 2.- $\frac{1}{14}$-scale model of the XB-36 outboard nacelle; configuration 1.

NATIONAL ADVISORY COMMITTEE FOR AERONAUTICS
LANGLEY MEMORIAL AERONAUTICAL LABORATORY LANGLEY FIELD VA

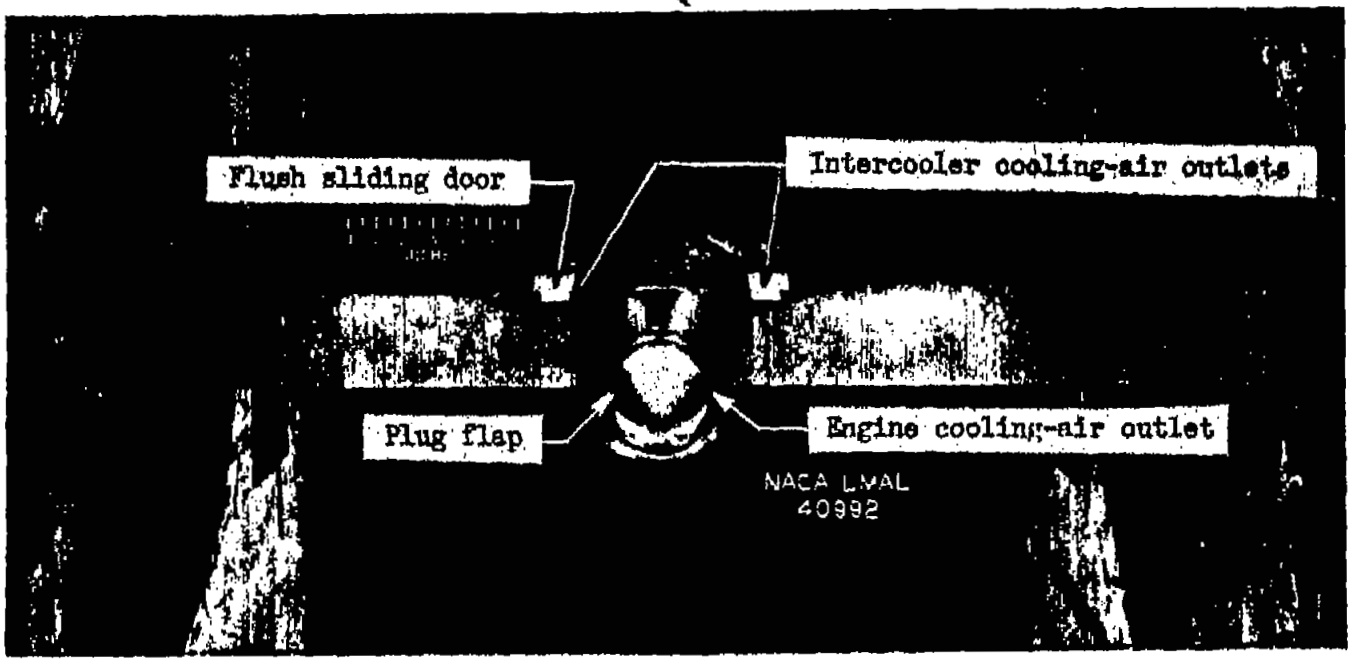

(b) Rear top view showing cooling-air outlets.

Figure 2.- Continued.

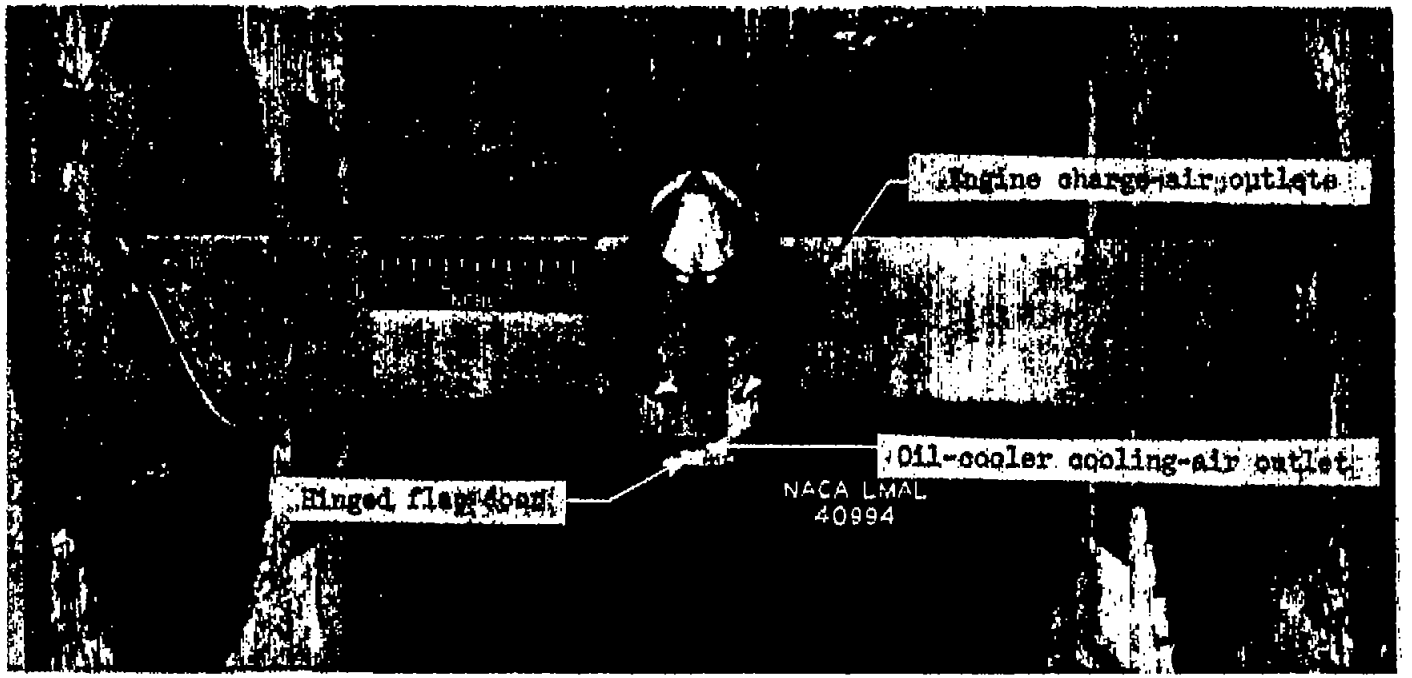

(c) Rear bottom view showing air outlets.

Figure 2.- Concluded.

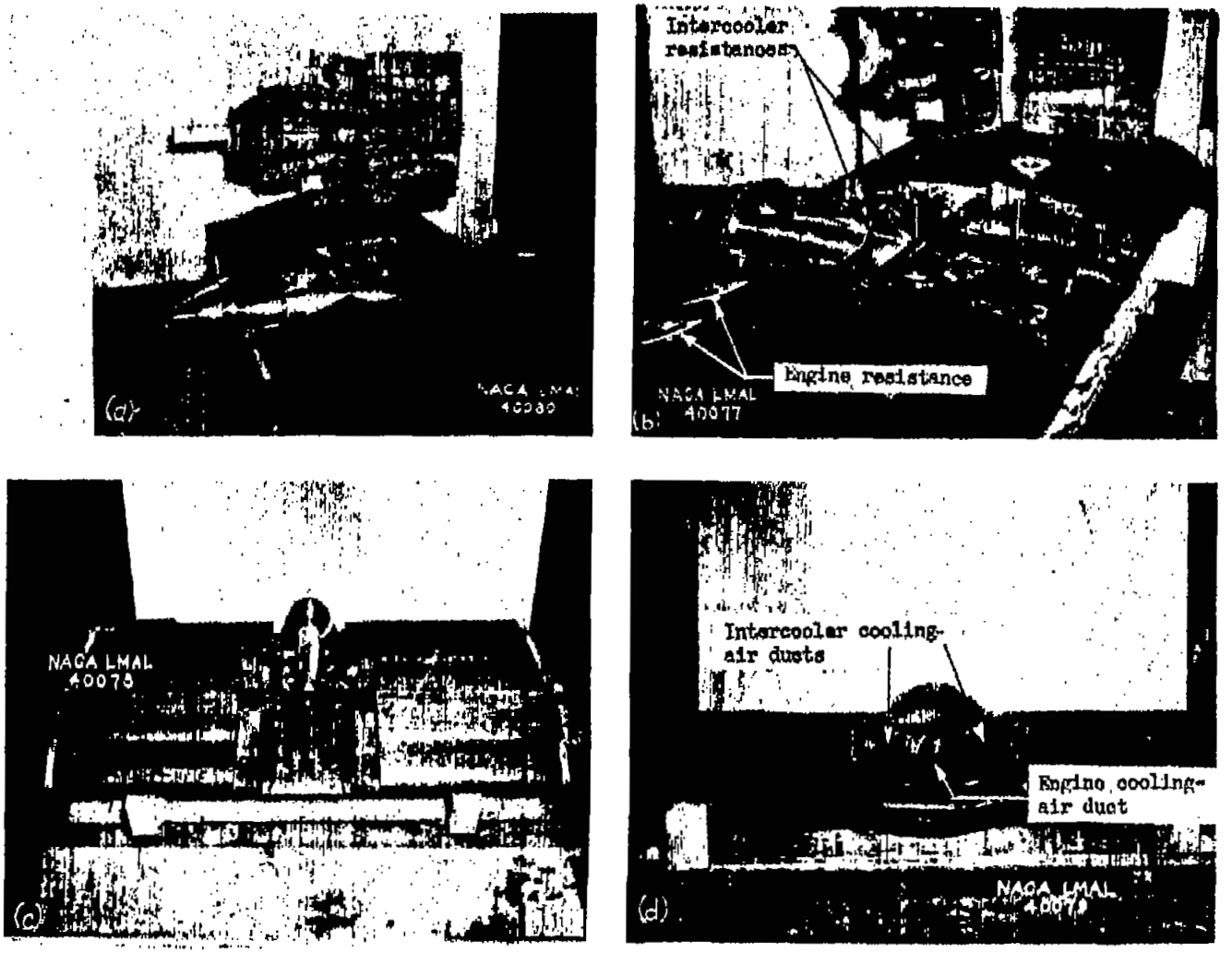

Figure 3.- Various views of parts of $\frac{1}{14}$-scale model of XB-36 outboard nacelle; configuration 1.

NATIONAL ADVISORY COMMITTEE FOR AERONAUTICS
LANGLEY MEMORIAL AERONAUTICAL LABORATORY - LANGLEY FIELD, VA

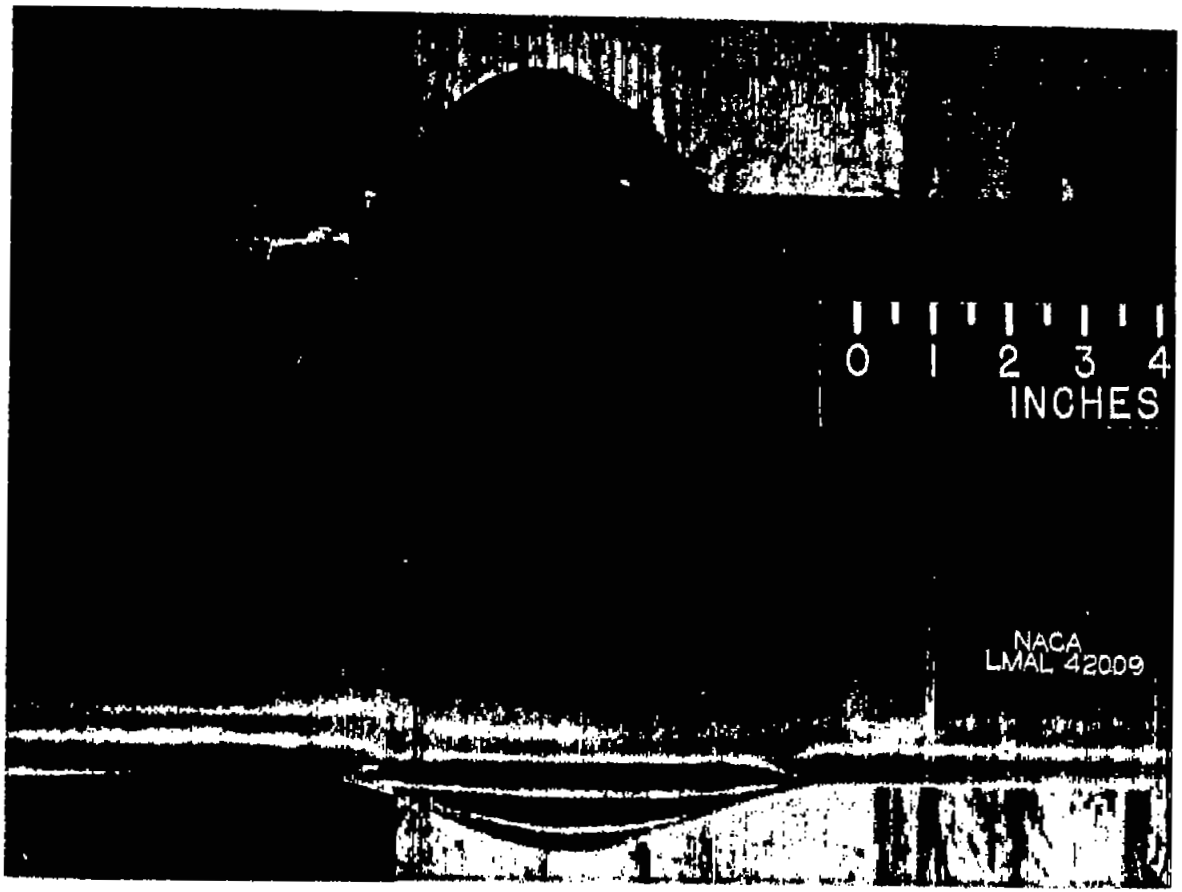

(a) Front top view showing small beaver tail fairing.

Figure 4.- $\frac{1}{14}$-scale model of XB-36 outboard nacelle with external fairings; configuration 1.

NATIONAL ADVISORY COMMITTEE FOR AERONAUTICS
LANGLEY MEMORIAL AERONAUTICAL LABORATORY LANGLEY FIELD VA

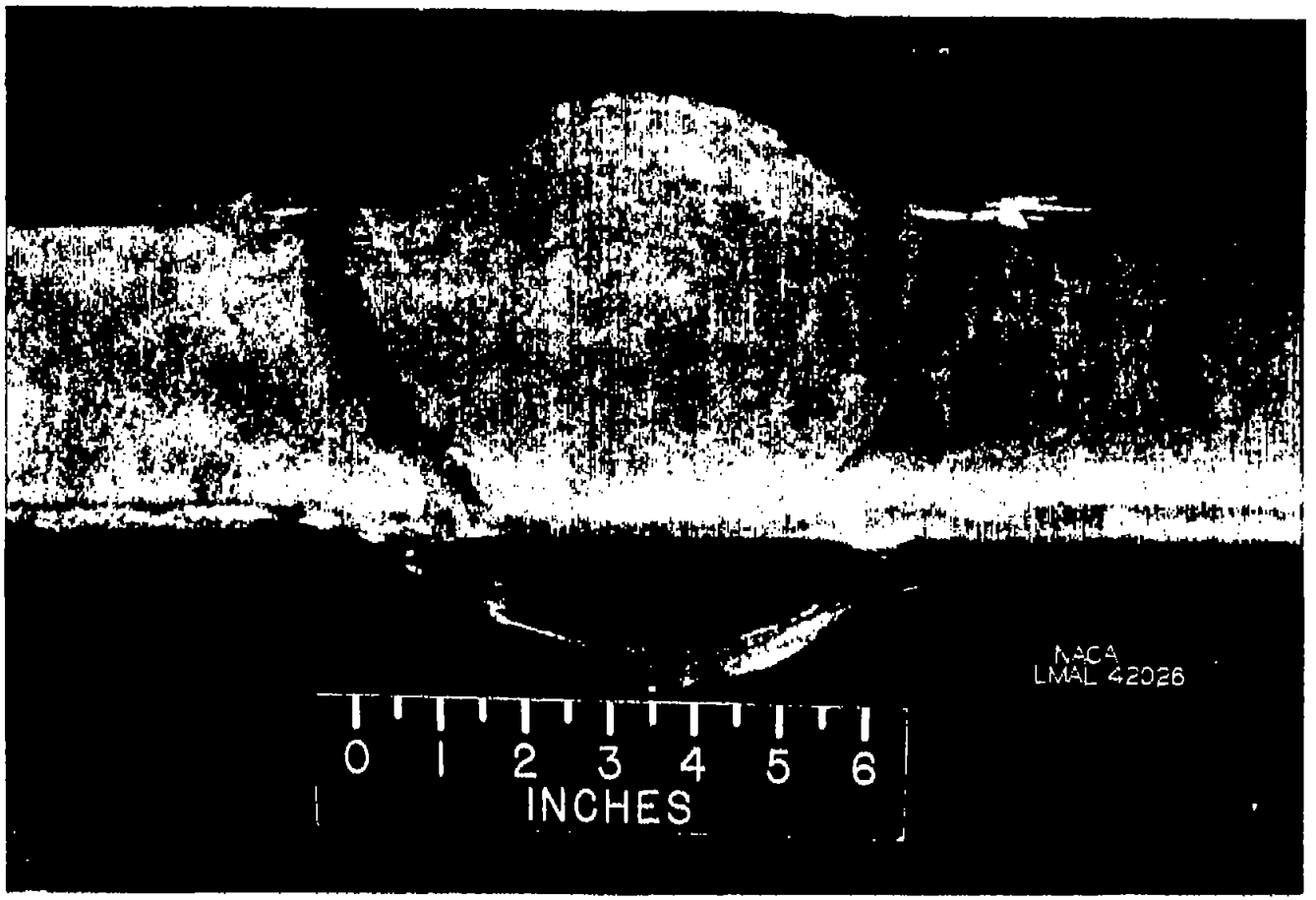

(b) Front top view showing large beaver tail fairing.

Figure 4.- Continued.

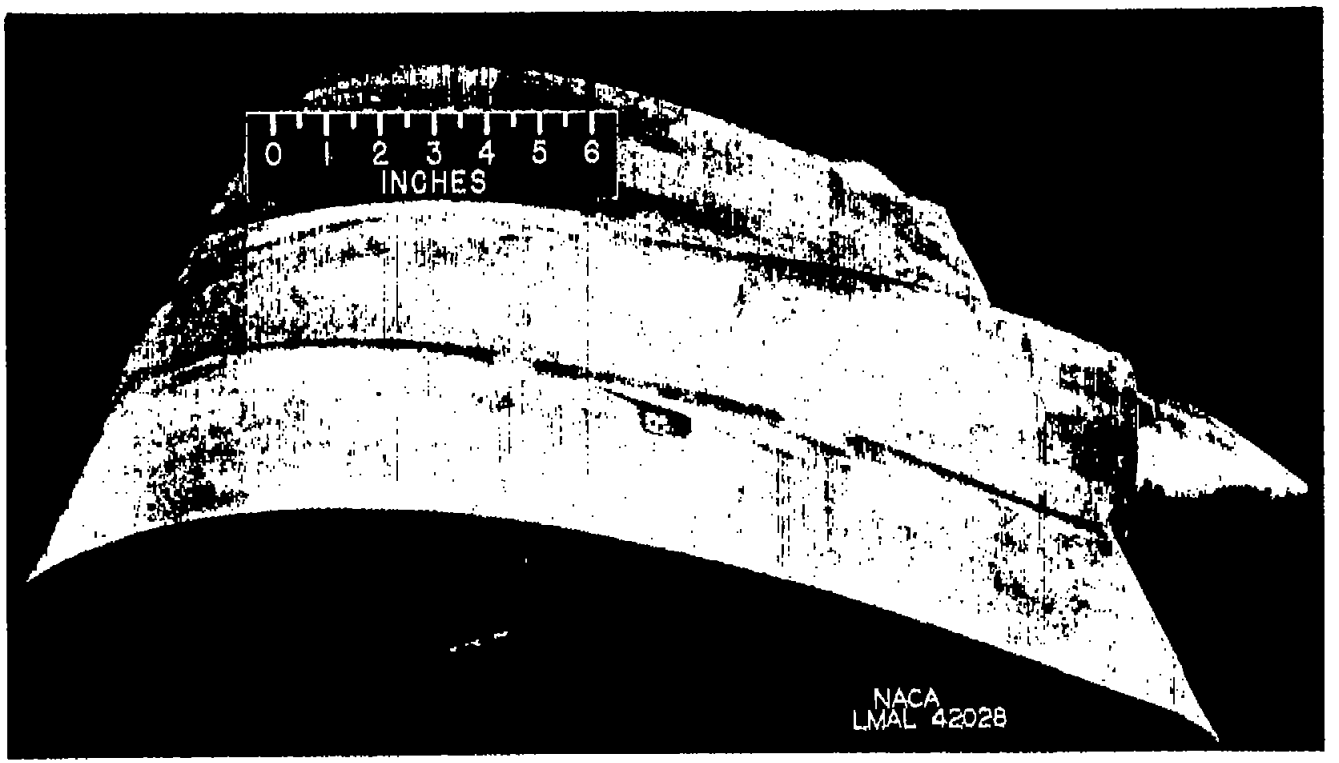

(c) Profile view showing large beaver tail fairing and wing-nacelle fillet.

Figure 4.- Concluded.

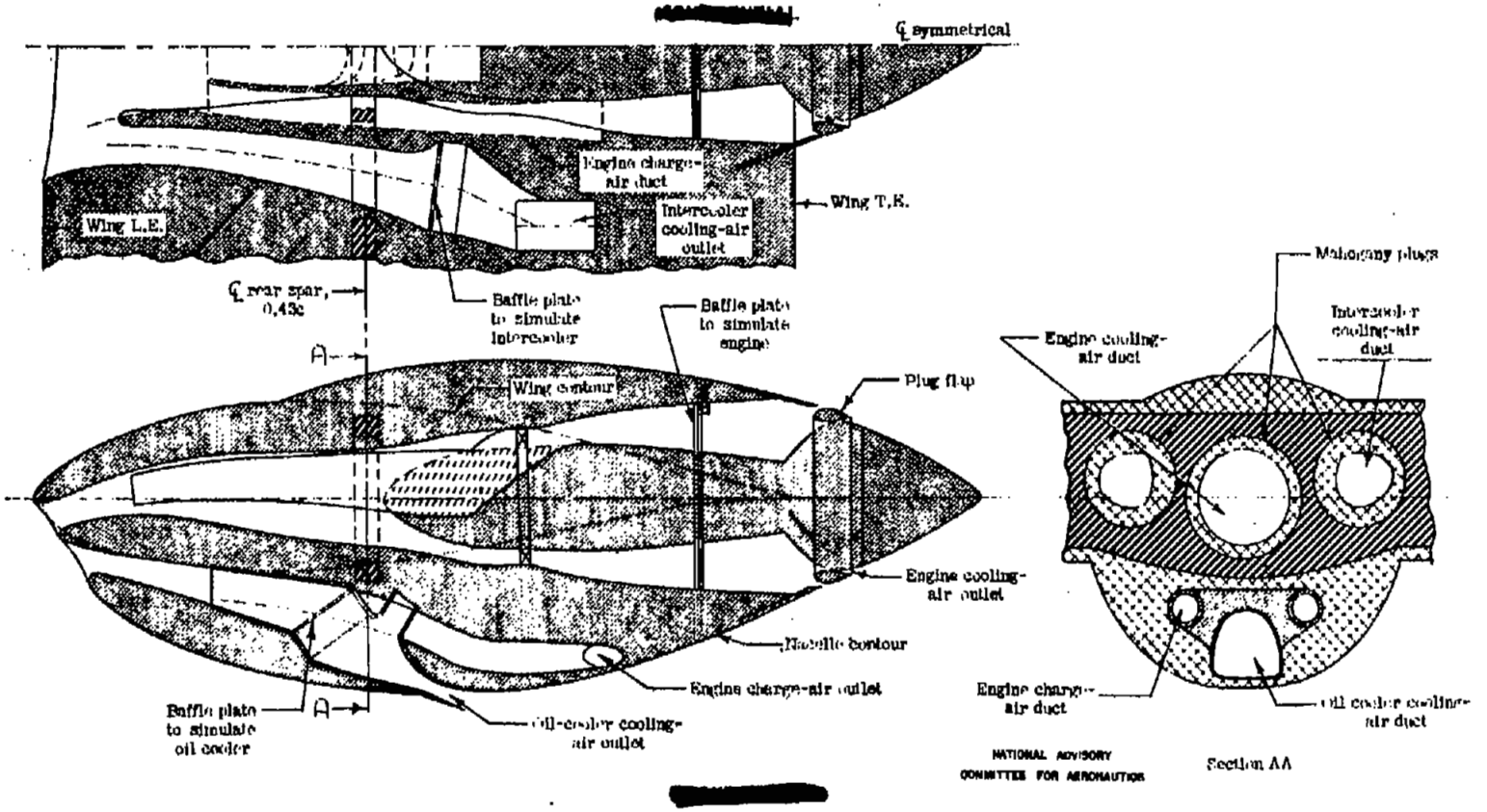

Figure 5.- General arrangement of $\frac{1}{14}$-scale model of XB-38 outboard nacelle; configuration 2.

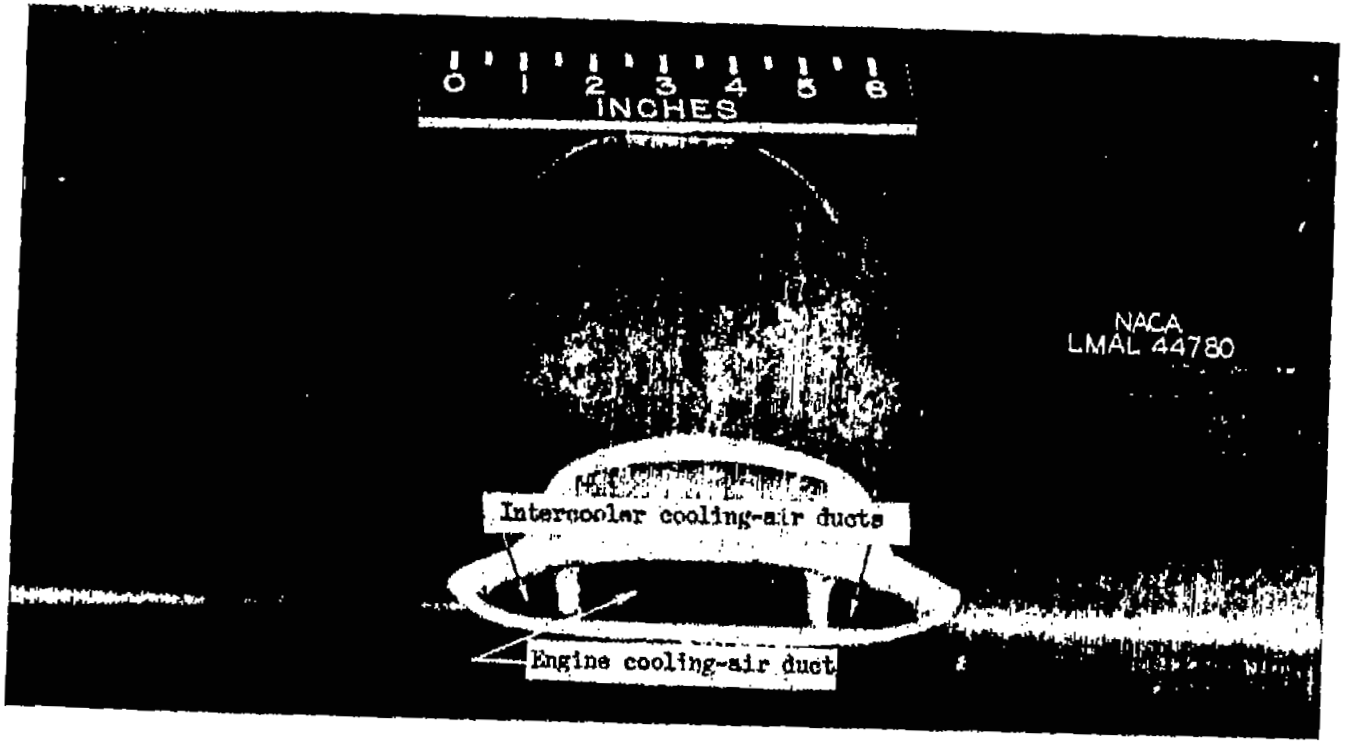

(a) Front view showing leading-edge air inlet (model inverted).

Figure 6.- $\frac{1}{14}$-scale model of XB-36 outboard nacelle; configuration 2.

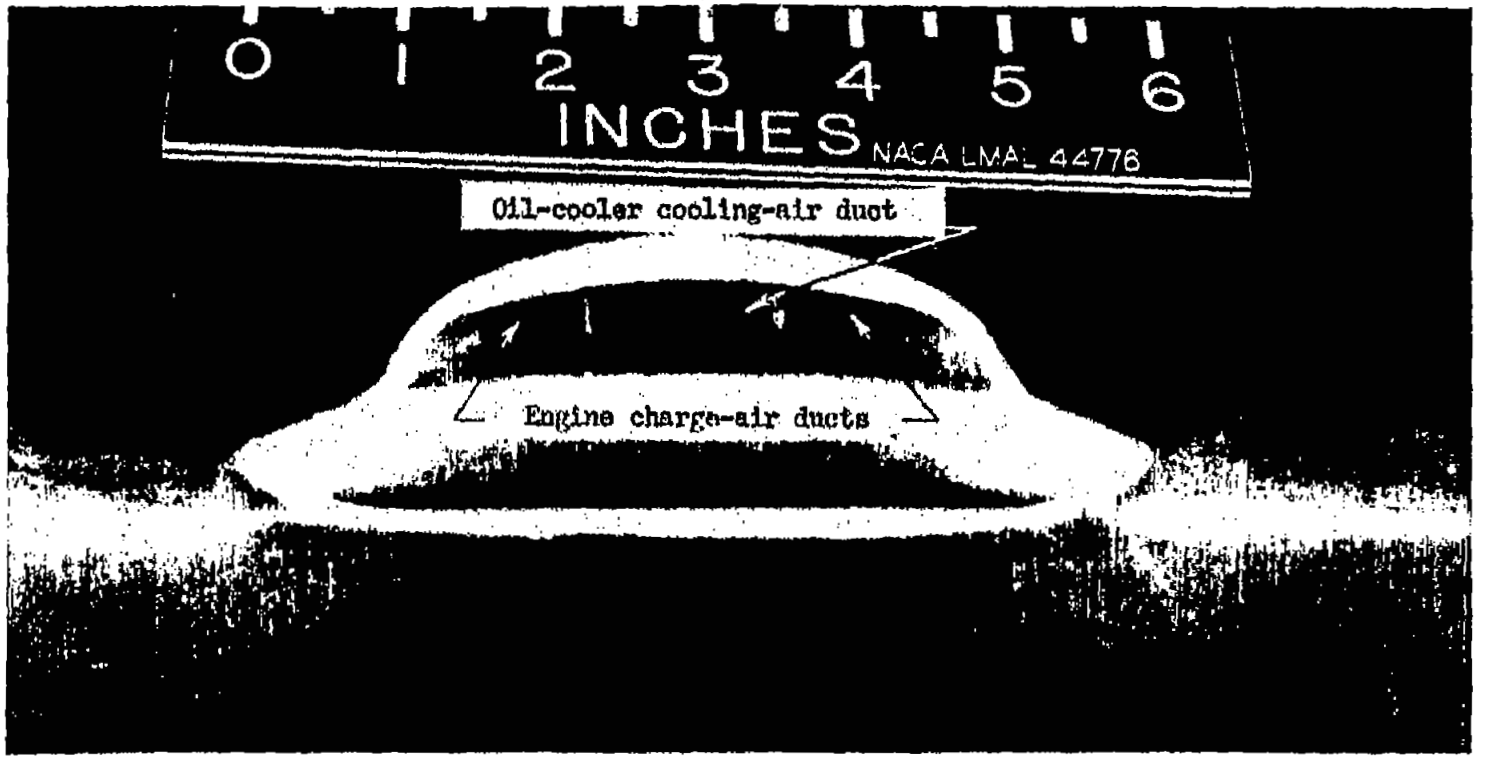

(b) Front view showing underwing air inlet (model inverted).

Figure 6.- Continued.

NATIONAL ADVISORY COMMITTEE FOR AERONAUTICS
LANGLEY MEMORIAL AERONAUTICAL LABORATORY LANGLEY FIELD VA

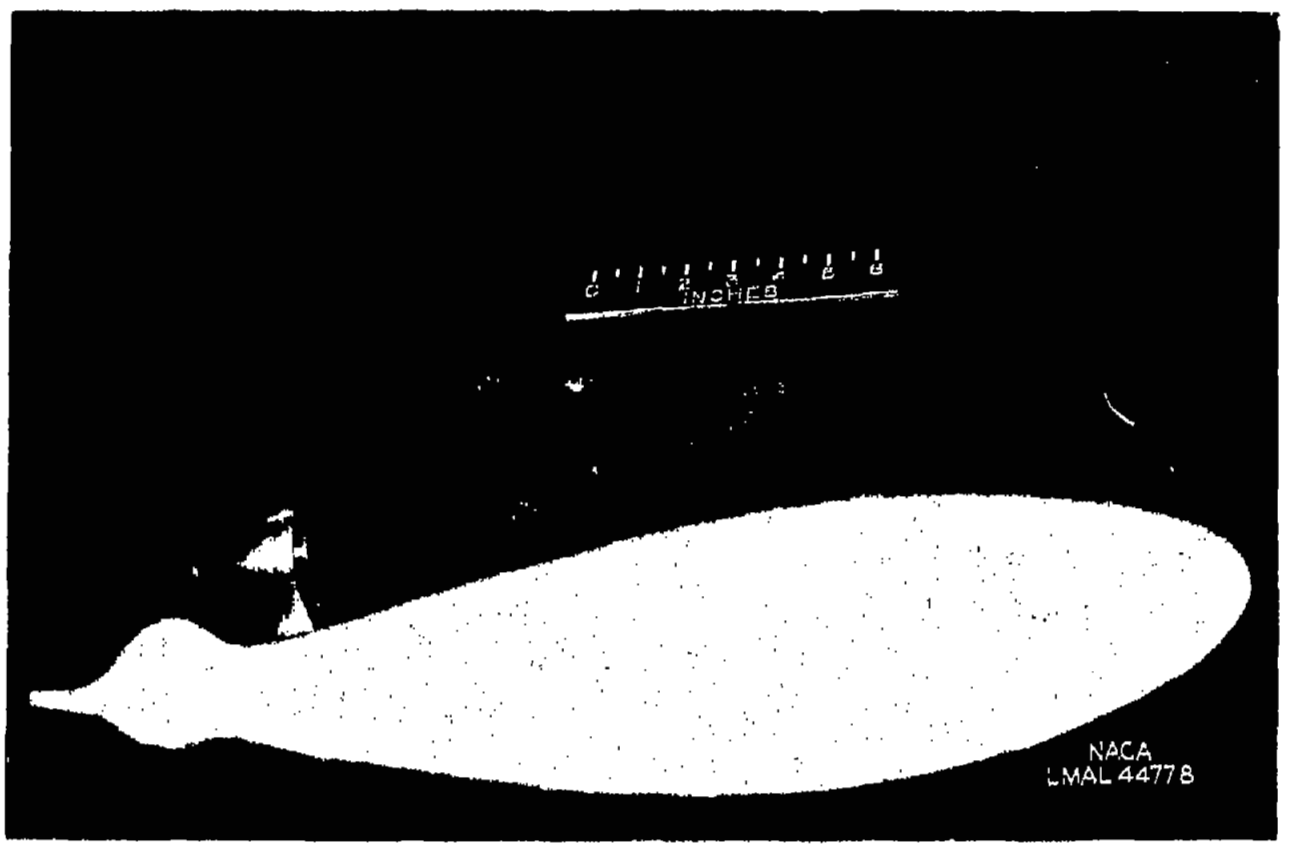

(c) Profile of model inverted.

Figure 6.- Concluded.

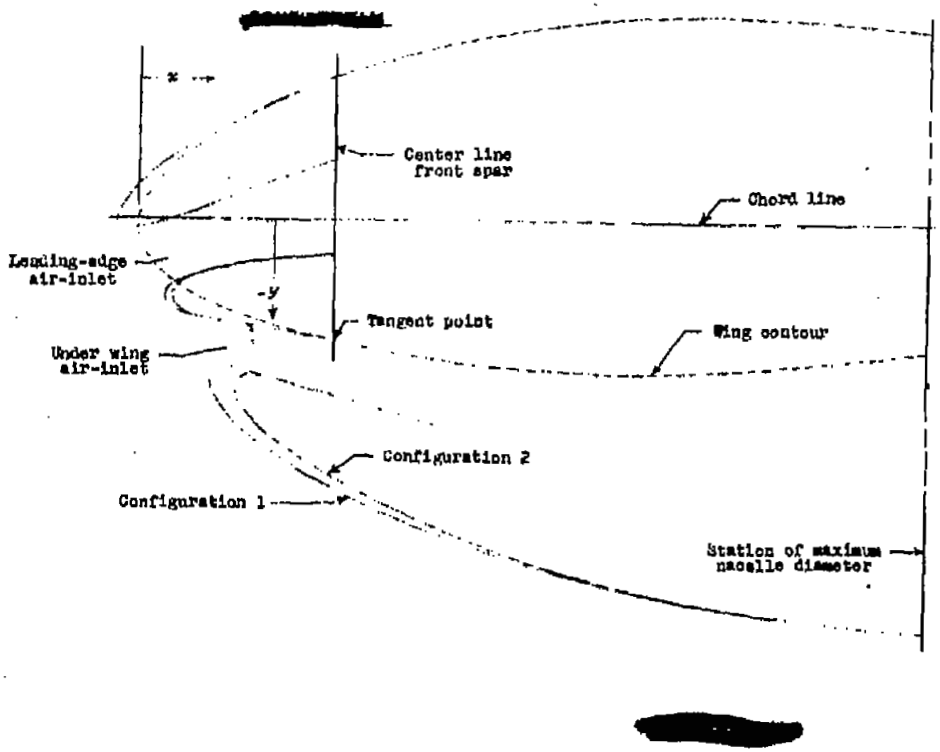

LOCATION AND MAGNITUDE OF LIP RADII ALONG CENTER LINE OF XB-36 OUTBOARD NACELLE MODELS (percent of airfoil chord)

Configuration	Leading-edge air-inlet			
	Lip radius		Radius center at	
	Upper	Lower	Upper	Lower
1	0.436	0.684	-x = 0.873 -y = .055	x = 2.266 -y = 4.416
2	.436	.782	-x = 0.873 -y = .055	x = 2.340 -y = 4.398

Configuration	Under wing air-inlet	
	Lip radius	Radius center at
1	0.819	x = 5.210 -y = 9.346
2	.992	x = 6.872 -y = 9.914

NATIONAL ADVISORY COMMITTEE FOR AERONAUTICS

Figure 7.- Profile of air inlets of configurations 1 and 2; center line of 1/14-scale model of XB-36 outboard nacelle.

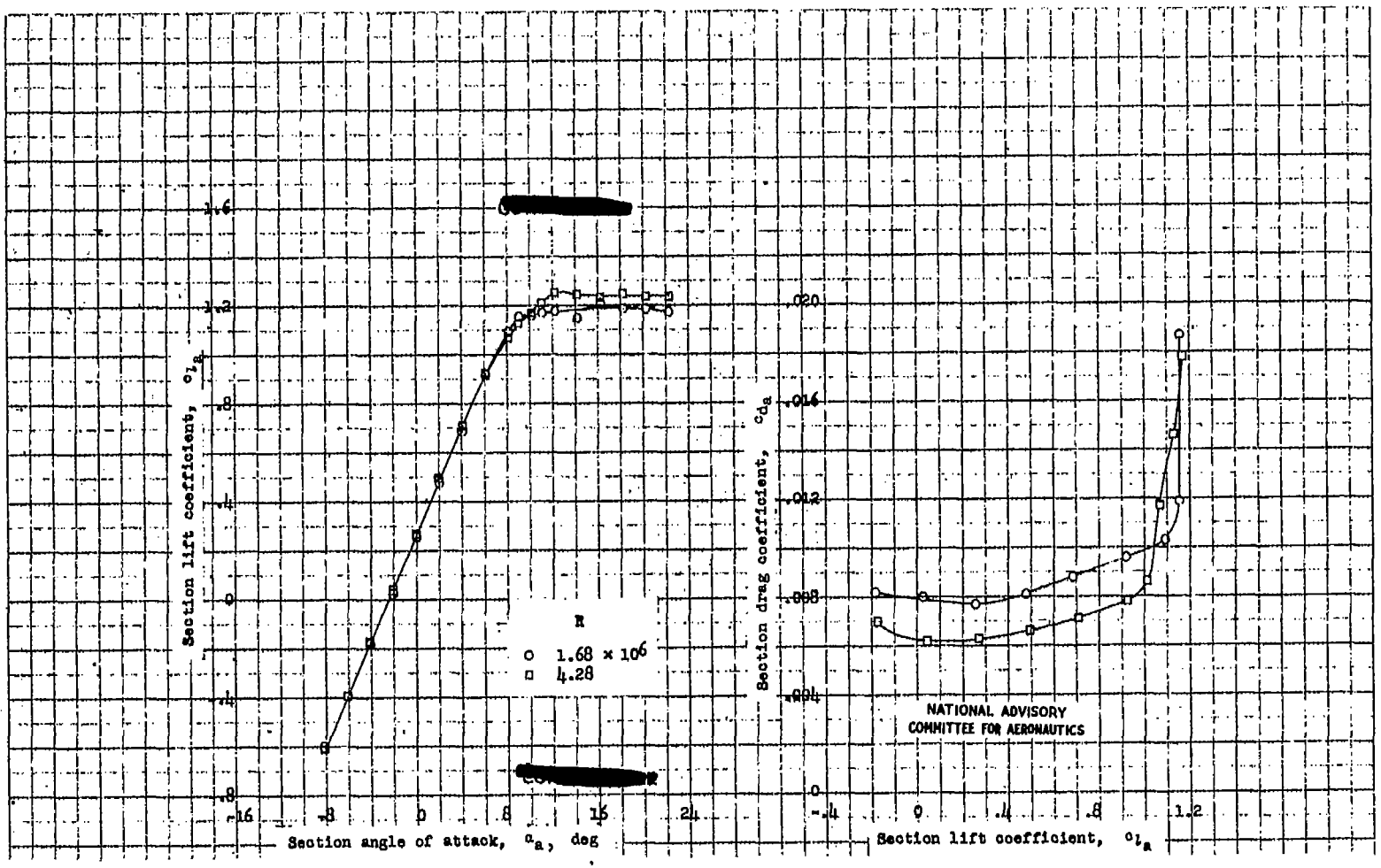

Figure 8.- Aerodynamic characteristics of a 16.371-inch chord NACA 63(420)-4(20.7) (approximately) airfoil; 1/14-scale model of XB-36 outboard wing panel (station 786).

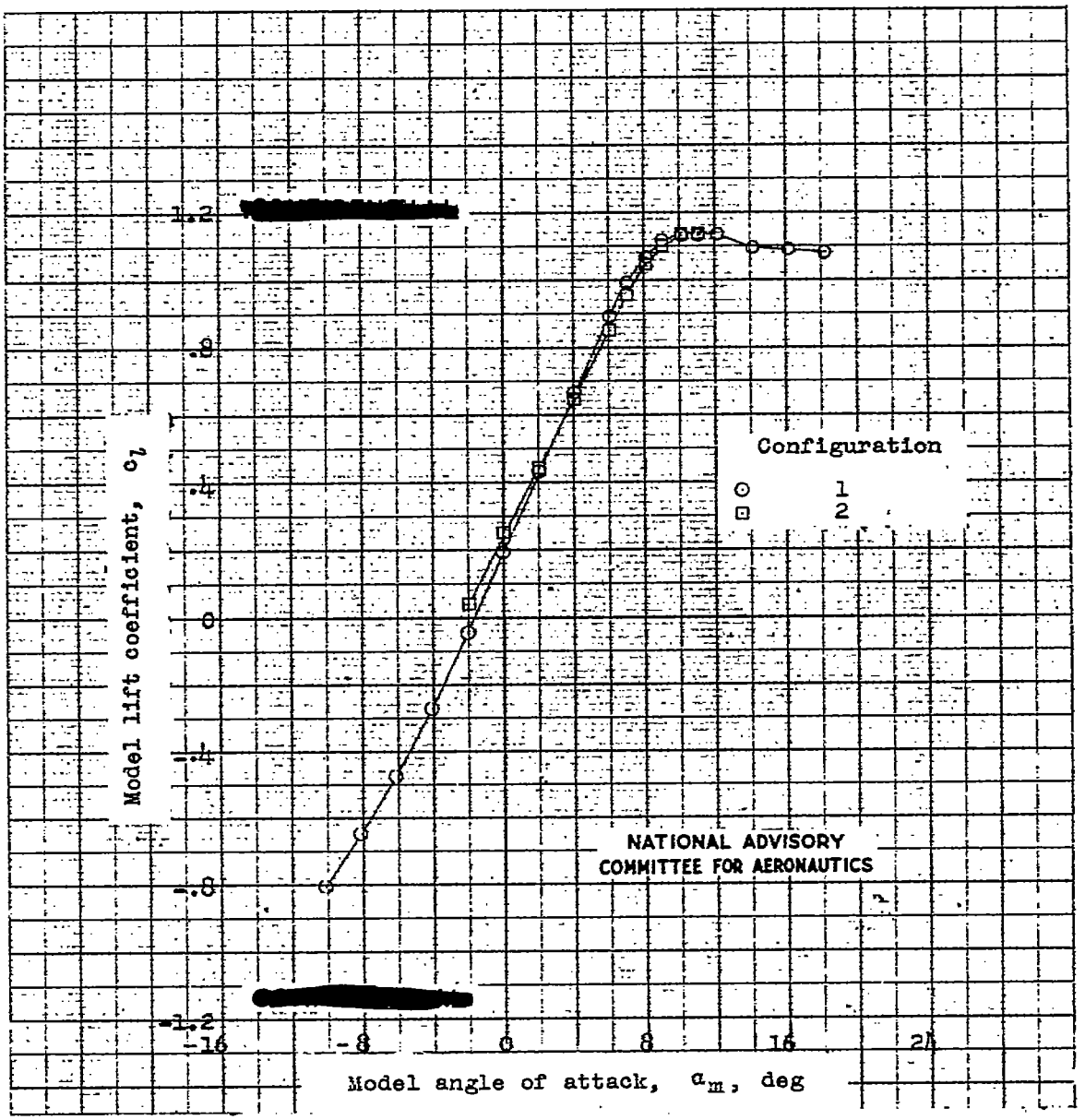

Figure 9.- Lift characteristics of 1/14-scale models of the XB-36 outboard nacelle. No baffles, duct exits approximately half open; $R \cong 1.68 \times 10^6$.

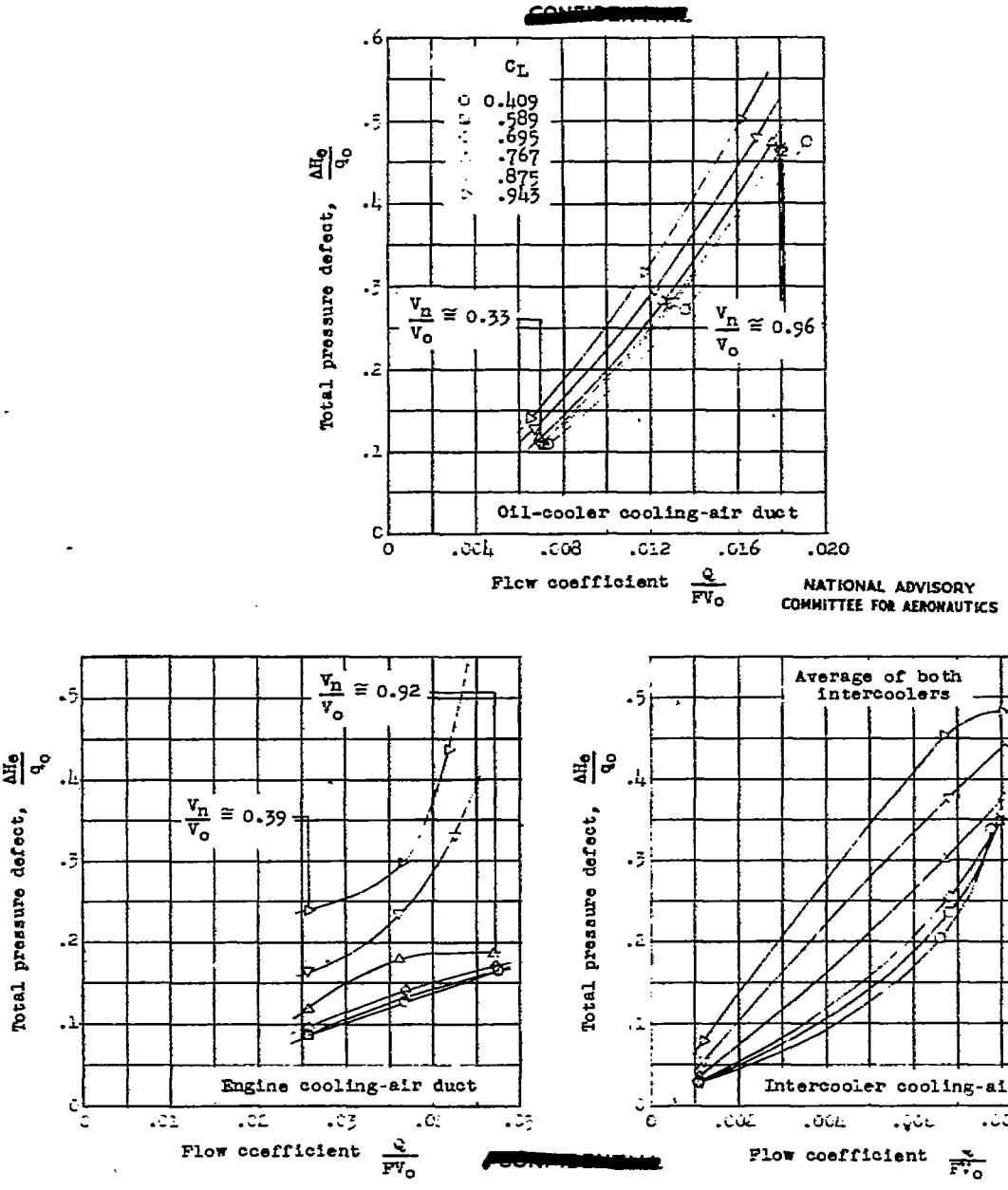

Figure 10.- Variation of total pressure defect at the cooling air duct exits with flow coefficient for 1/14-scale model of XB-36 outboard nacelle. Configuration 1; runs 1 to 3; no baffles; $R \cong 1.68 \times 10^6$.

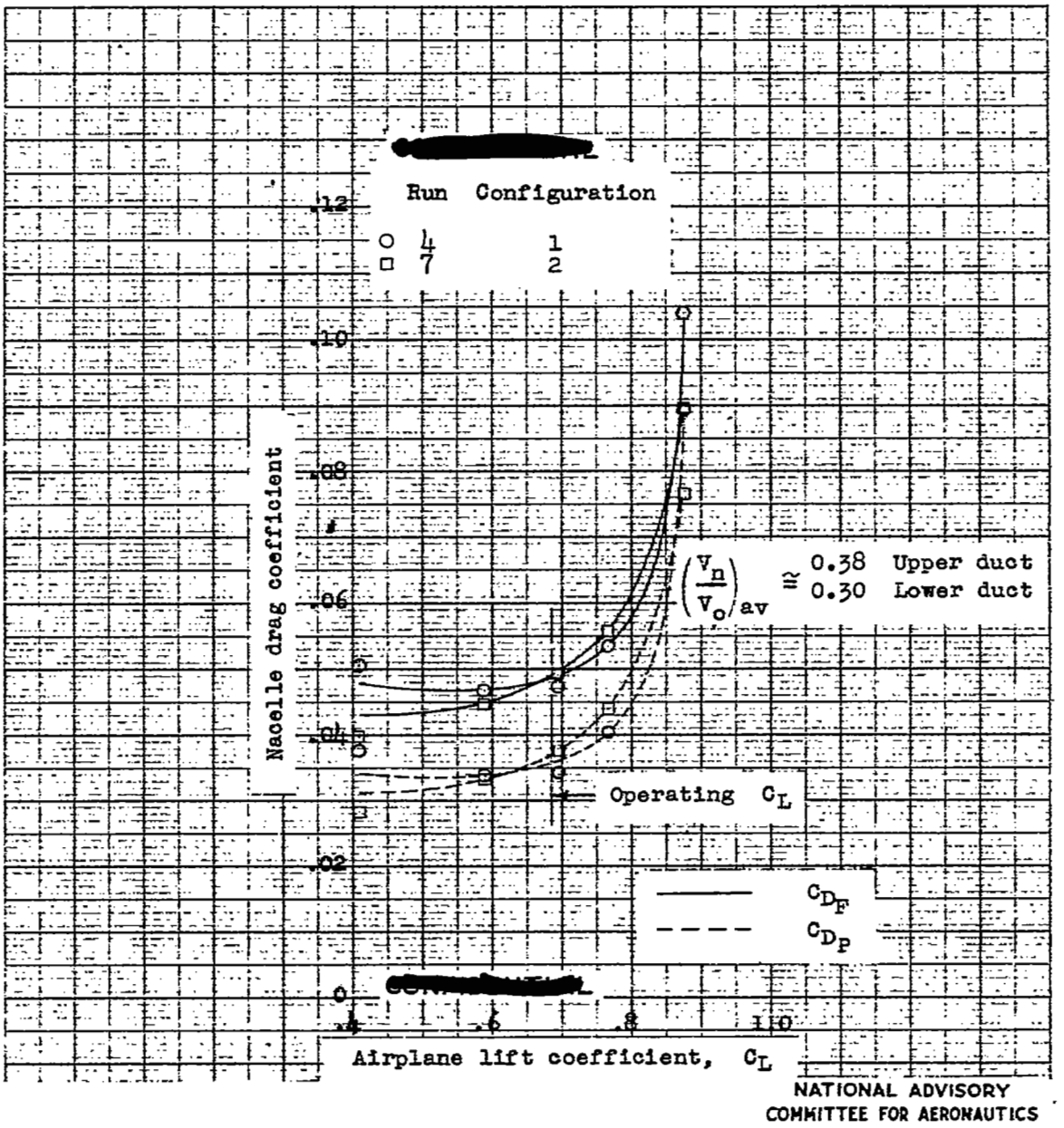

Figure 11.- Drag characteristics of 1/14-scale model of XB-36 outboard nacelle (exclusive of engine charge air) based on model nacelle frontal area. Cruise condition at 10,000 feet; $R \cong 1.68 \times 10^6$.

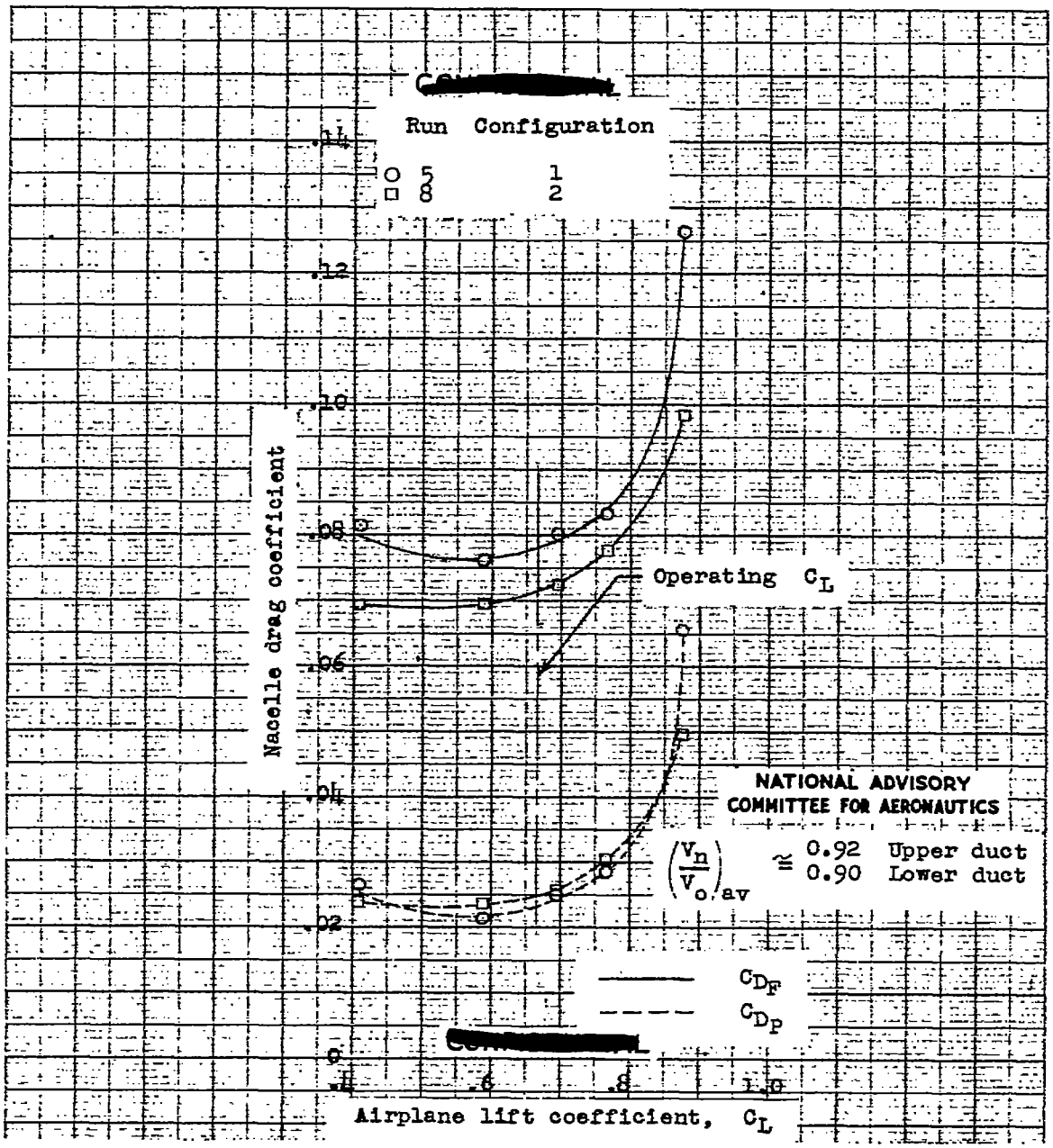

Figure 12.- Drag characteristics of 1/14-scale model of XB-36 outboard nacelle (exclusive of engine charge air) based on model nacelle frontal area. Cruise condition at 40,000 feet; $R \cong 1.68 \times 10^6$.

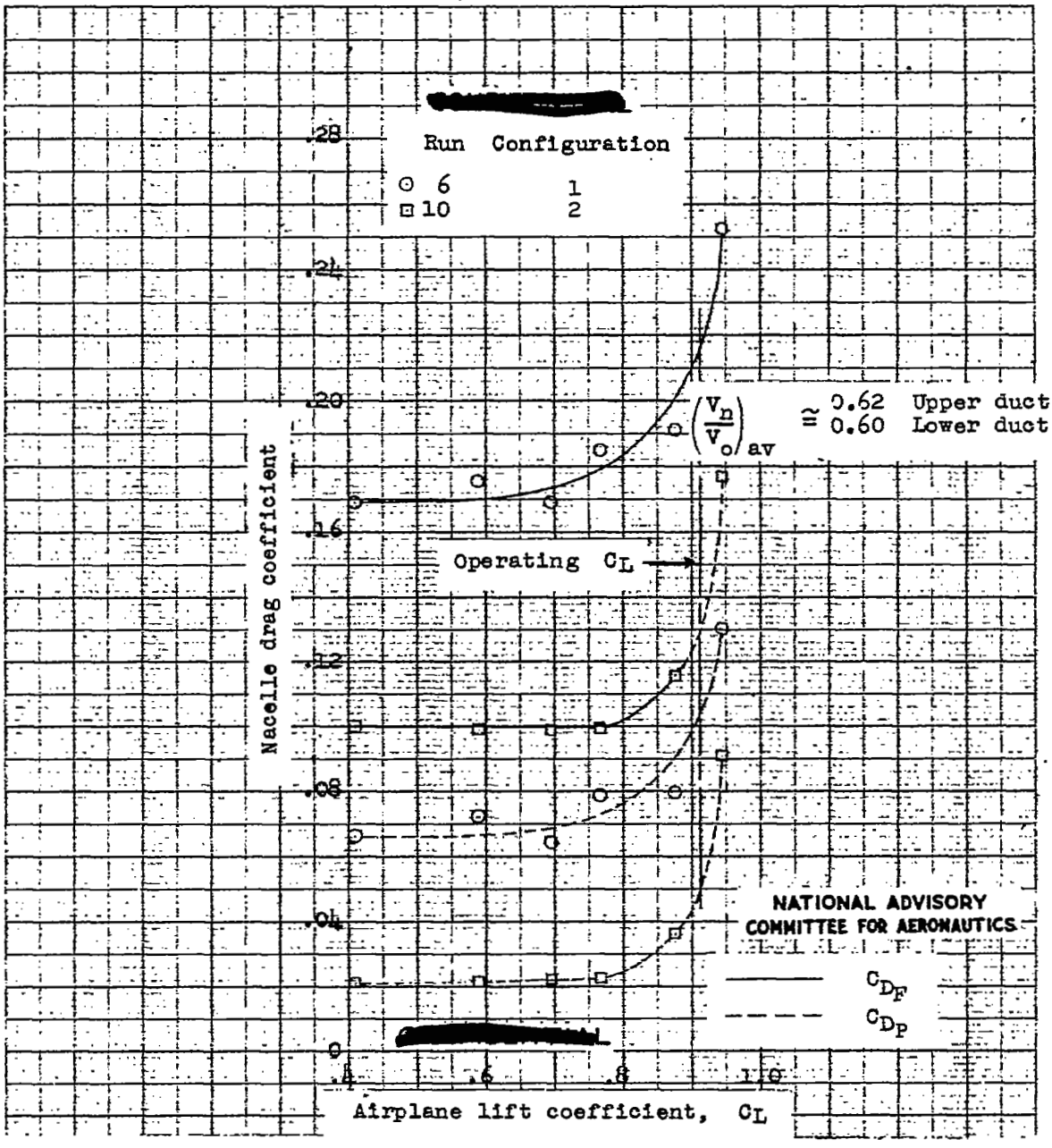

Figure 13.- Drag characteristics of 1/14-scale model of XB-36 outboard nacelle (exclusive of engine charge air) based on model nacelle frontal area. Climb condition at 40,000 feet; $R \cong 1.68 \times 10^6$.

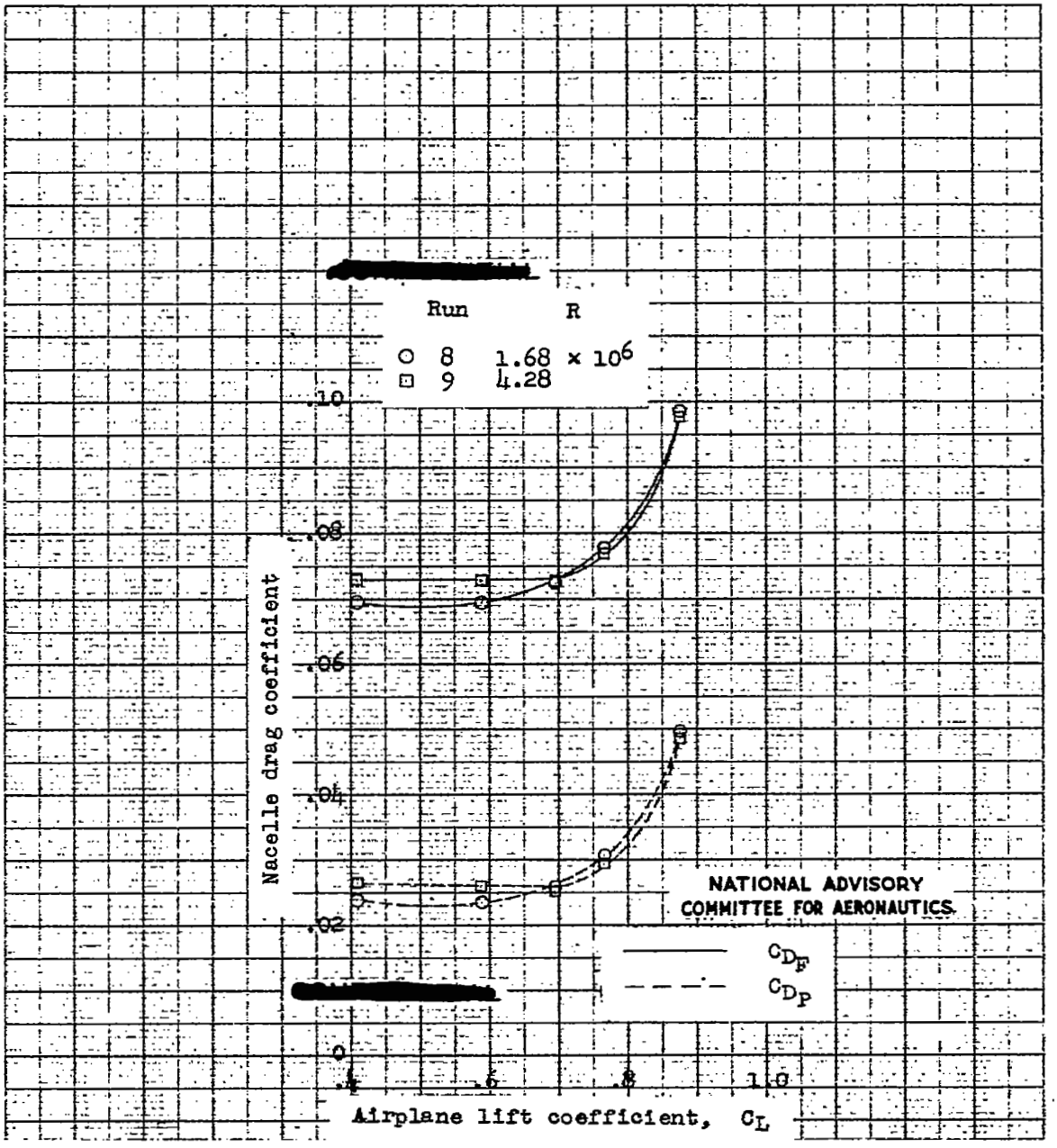

Figure 14.- Drag scale effect of 1/14-scale model of XB-36 outboard nacelle (exclusive of engine charge air) based on model nacelle frontal area. Configuration 2; cruise condition at 40,000 feet.

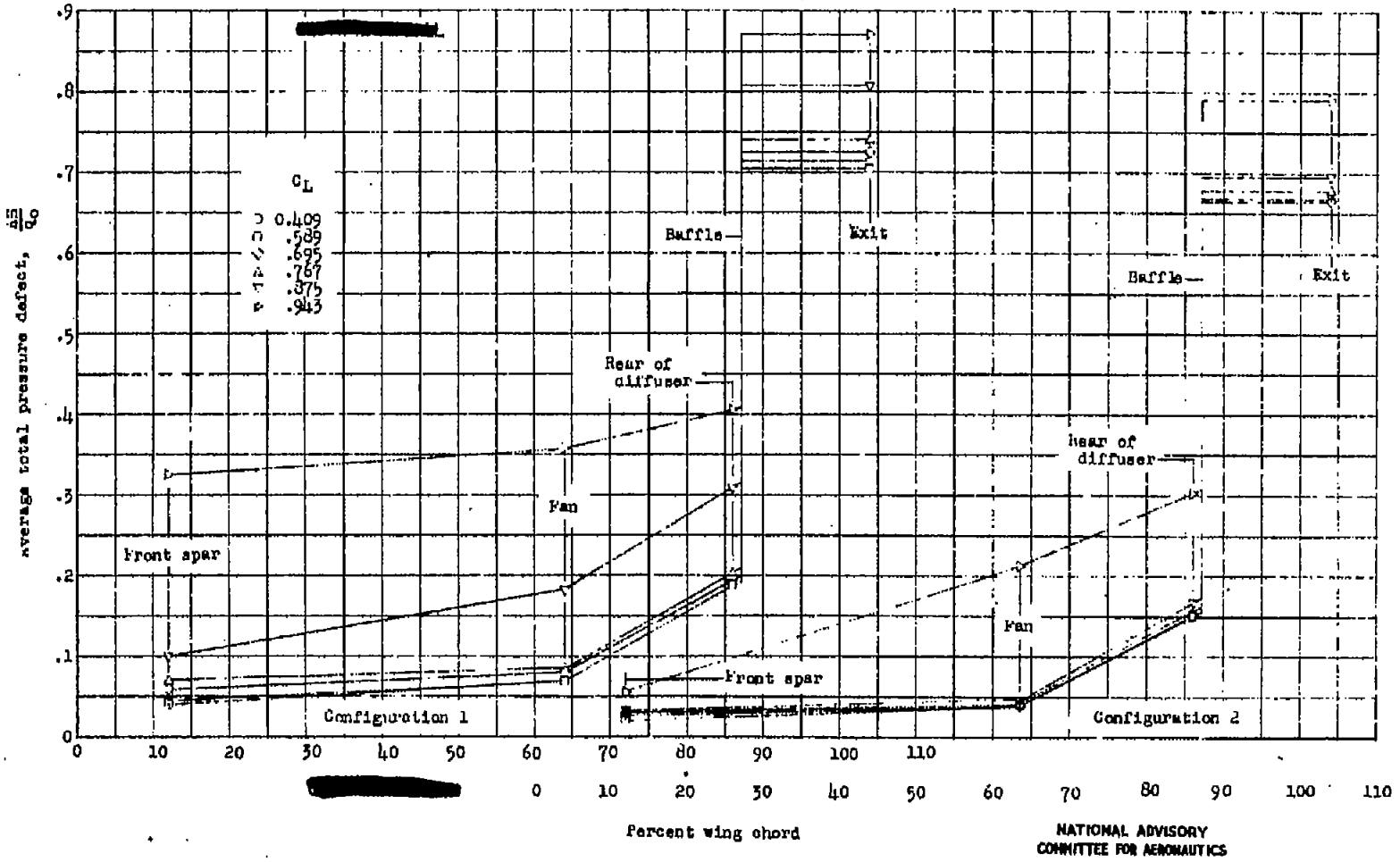

(a) Engine cooling-air duct.

Figure 15.- Average total pressure defect at several chordwise positions within the cooling-air duct; 1/14-scale model of the XB-36 outboard nacelle. Climb condition at 40,000 feet; $R \cong 1.68 \times 10^6$.

Fig. 15a

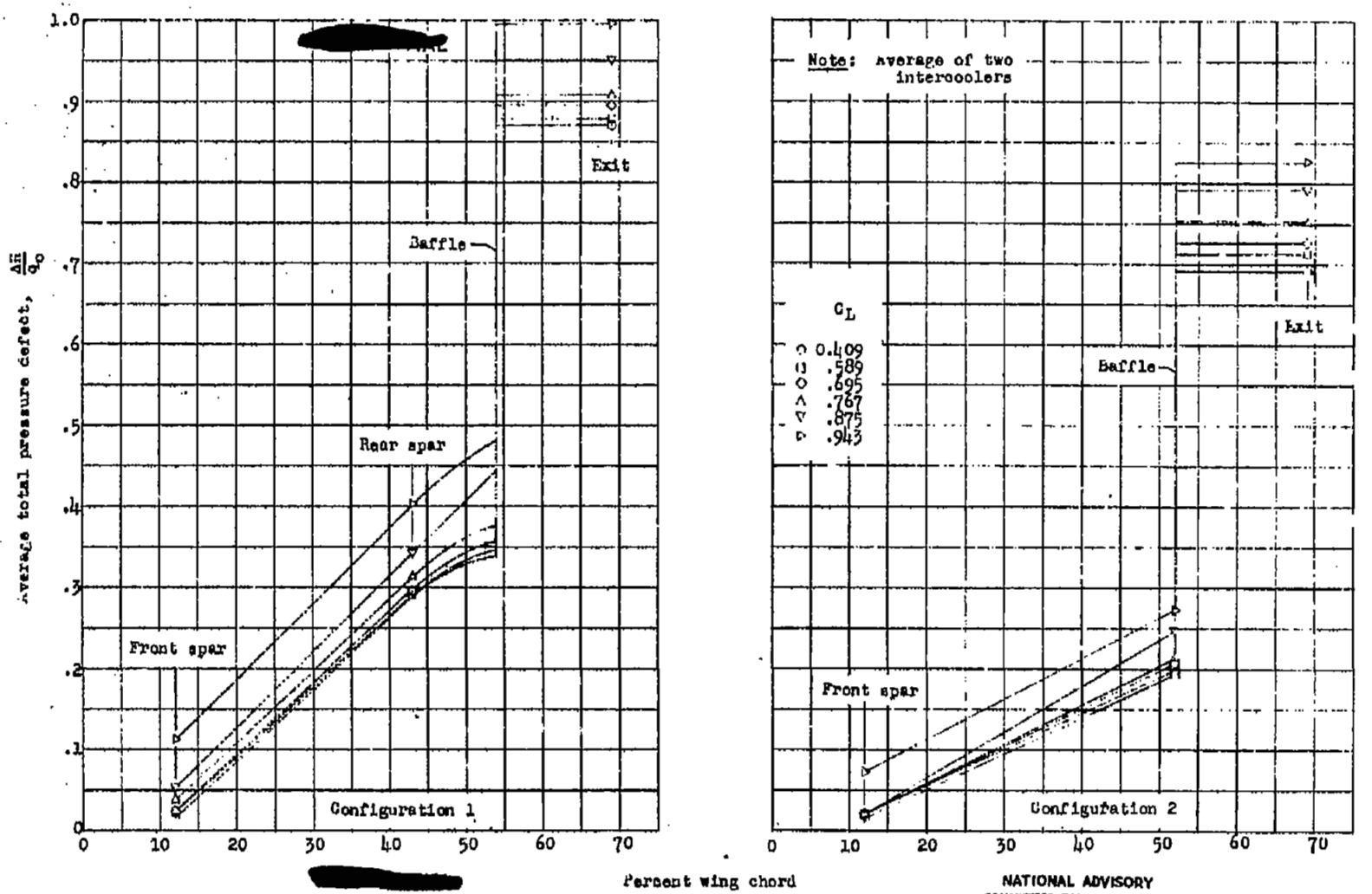

(b) Intercooler cooling-air ducts.

Figure 15.- Continued.

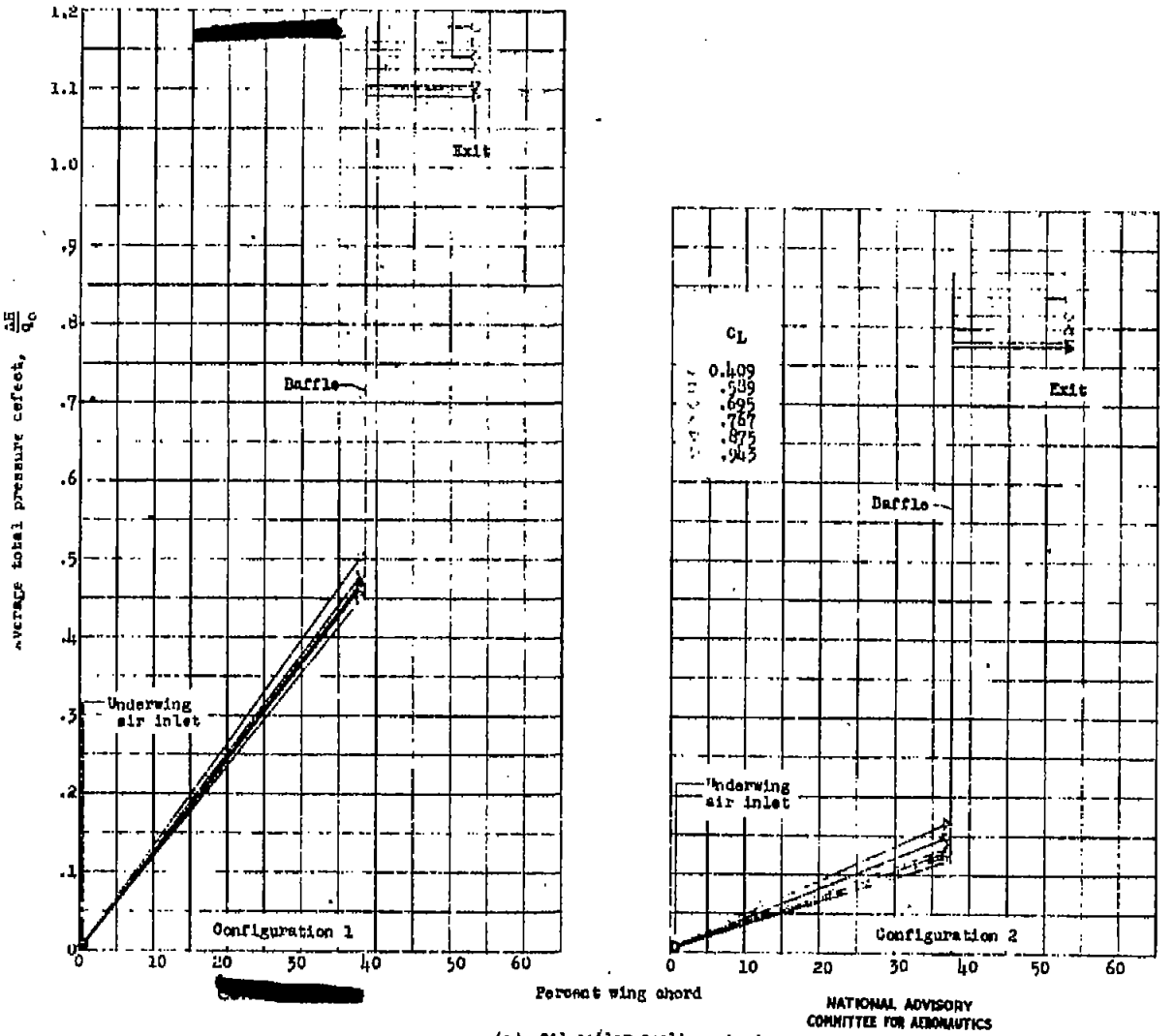

(a) Oil-cooler cooling-air duct.

Figure 15.- Concluded.